US 20240060164A1

(19) **United States**

(12) **Patent Application Publication**

BRADY et al.

(10) **Pub. No.: US 2024/0060164 A1**

(43) **Pub. Date: Feb. 22, 2024**

(54) **CAST IRON-BASE, HIGH-STRENGTH, OXIDATION-RESISTANT ALLOY**

(71) Applicant: **UT-BATTELLE, LLC**, Oak Ridge, TN (US)

(72) Inventors: **MICHAEL P. BRADY**, Oak Ridge, TN (US); **GOVINDARAJAN MURALIDHARAN**, Knoxville, TN (US); **YUKINORI YAMAMOTO**, Knoxville, TN (US)

(21) Appl. No.: **18/236,326**

(22) Filed: **Aug. 21, 2023**

Related U.S. Application Data

(60) Provisional application No. 63/399,233, filed on Aug. 19, 2022.

Publication Classification

(51) **Int. Cl.**

C22C 38/58	(2006.01)
C22C 30/02	(2006.01)
C22C 38/54	(2006.01)
C22C 38/50	(2006.01)
C22C 38/48	(2006.01)
C22C 38/44	(2006.01)
C22C 38/42	(2006.01)
C22C 38/06	(2006.01)
C22C 38/04	(2006.01)
C22C 38/02	(2006.01)
C22C 38/00	(2006.01)

(52) **U.S. Cl.**

CPC ***C22C 38/58*** (2013.01); ***C22C 30/02*** (2013.01); ***C22C 38/54*** (2013.01); ***C22C 38/50*** (2013.01); ***C22C 38/48*** (2013.01); ***C22C 38/44*** (2013.01); ***C22C 38/42*** (2013.01); ***C22C 38/06*** (2013.01); ***C22C 38/04*** (2013.01); ***C22C 38/02*** (2013.01); ***C22C 38/005*** (2013.01)

(57) **ABSTRACT**

A cast AFA alloy composition comprising, in weight percent: 0.4 to 0.59 Nb+Ta; 0.4 to 0.6 C; 16 to 18 Cr; 18-23 Ni; 3.5-5.5 Al; 0.005 to 0.15 B; up to 1.5 Mo; up to 2 Co; up to 1 W; up to 3 Cu; up to 4 Mn; up to 2 Si; up to 0.5 wt. % total of at least one element selected from the group consisting of Ti and V; up to 0.06 N; up to 1 wt. % total of at least one element selected from the group consisting of Y, La, Ce, Hf, and Zr; balance Fe, wherein the weight percent Fe is greater than the weight percent Ni, and wherein the alloy forms an external continuous scale comprising alumina to at least 900° C. in air with 10% H_2O, and a stable essentially single-phase FCC austenitic matrix microstructure, the austenitic matrix being essentially delta-ferrite free and essentially BCC-phase-free, with creep rupture life in excess of 500 h at 900° C. and 50 MPa.

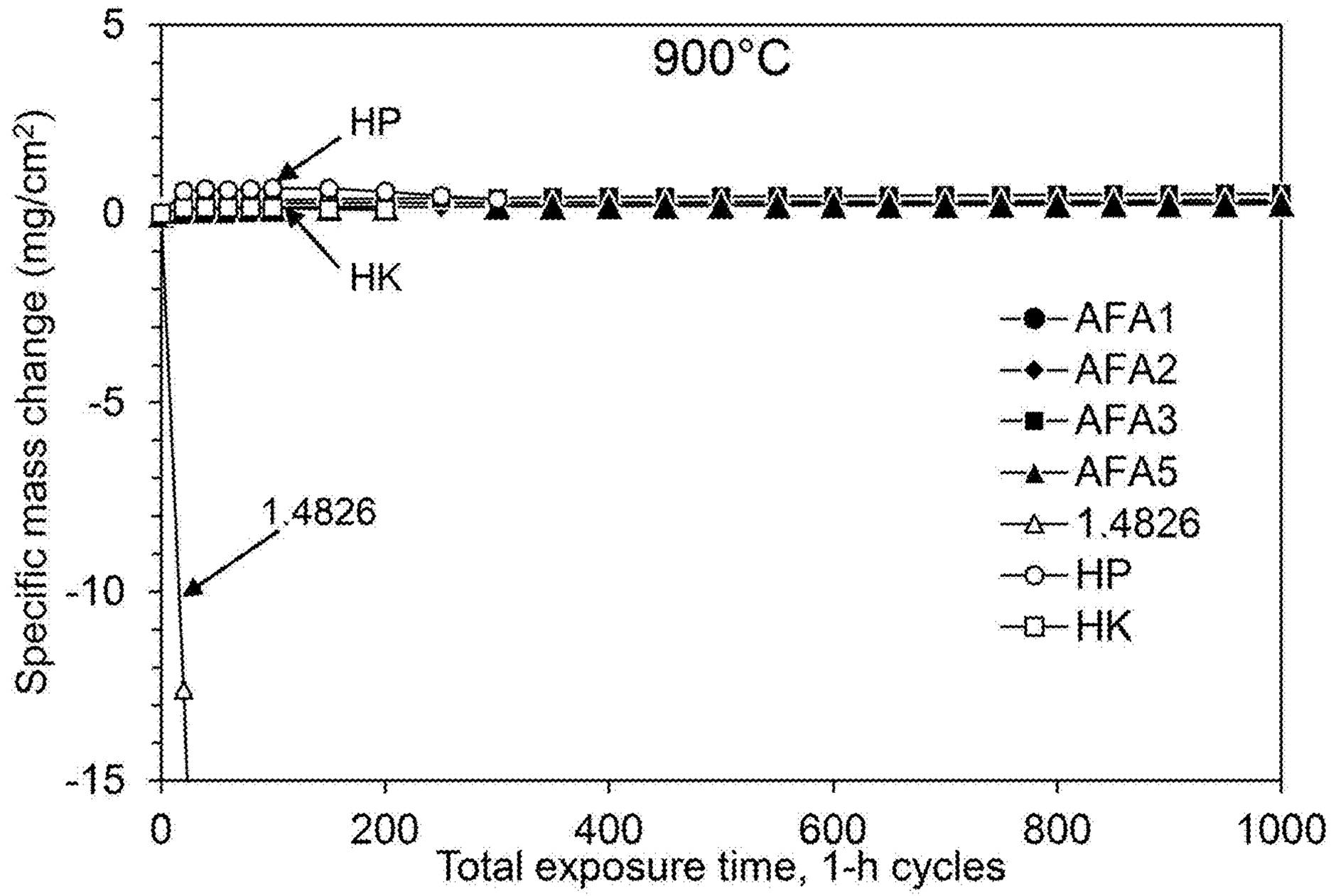
900°C
HP
HK
1.4826
AFA1
AFA2
AFA3
AFA5
1.4826
HP
HK
Specific mass change (mg/cm²)
5
0
-5
-10
-15
0
200
400
600
800
1000
Total exposure time, 1-h cycles

FIG. 1

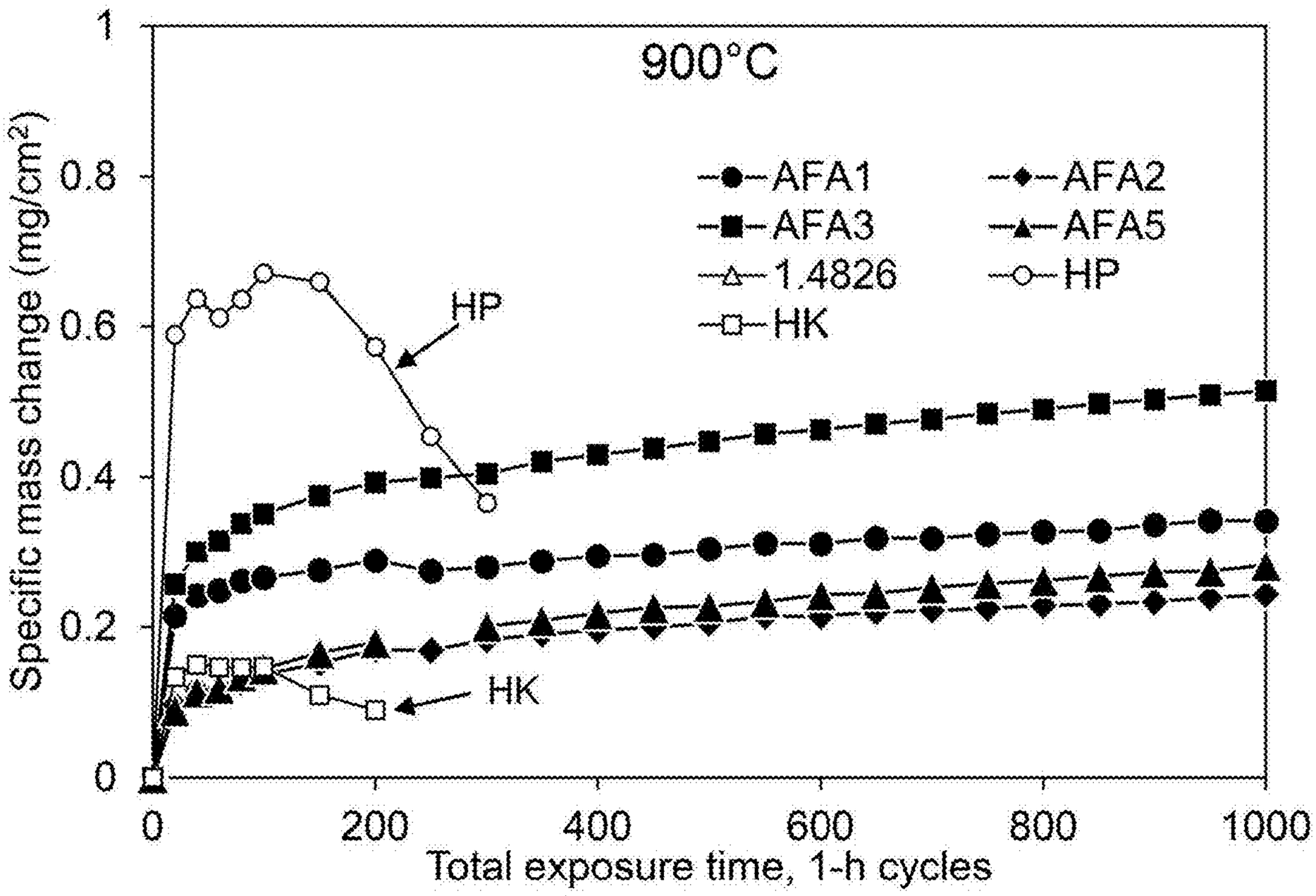
900°C
Specific mass change (mg/cm²)
Total exposure time, 1-h cycles
AFA1
AFA2
AFA3
AFA5
1.4826
HP
HK
HP
HK
0
0.2
0.4
0.6
0.8
1
0
200
400
600
800
1000

FIG. 2

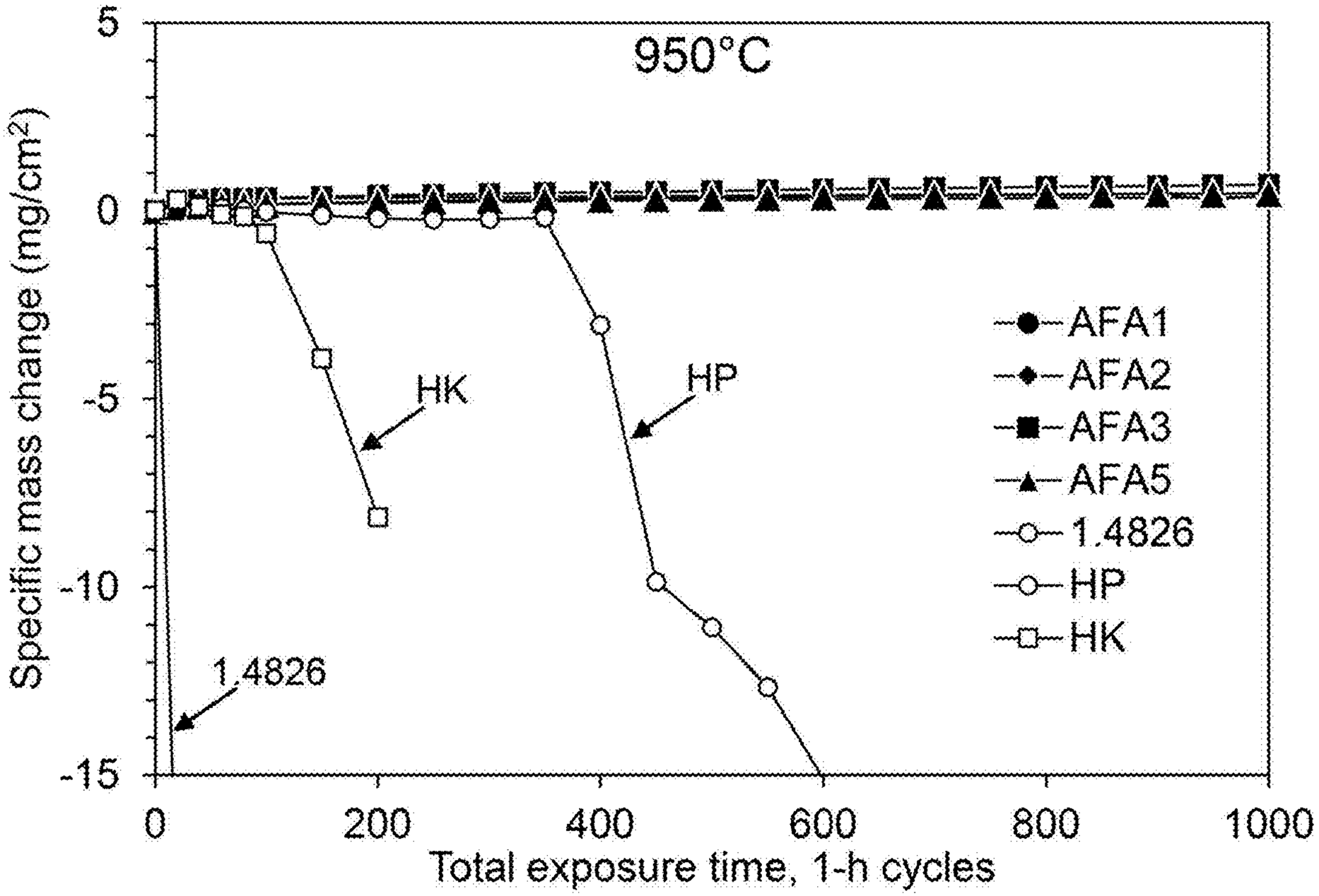
950°C
Specific mass change (mg/cm²)
5
0
-5
-10
-15
0
200
400
600
800
1000
Total exposure time, 1-h cycles
HK
HP
1.4826
AFA1
AFA2
AFA3
AFA5
1.4826
HP
HK

FIG. 3

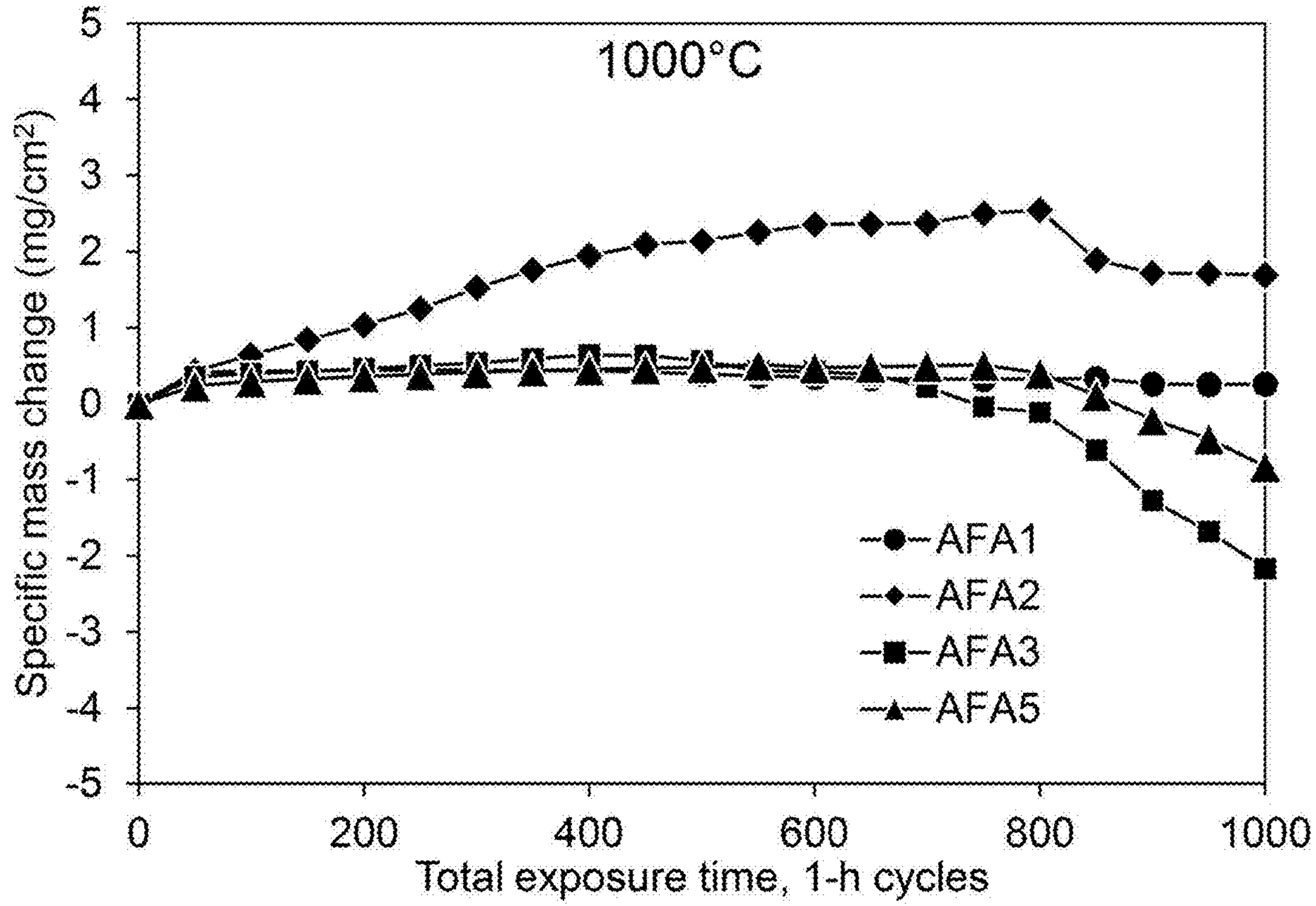
1000°C
Specific mass change (mg/cm²)
5
4
3
2
1
0
-1
-2
-3
-4
-5
0
200
400
600
800
1000
Total exposure time, 1-h cycles
AFA1
AFA2
AFA3
AFA5

FIG. 4

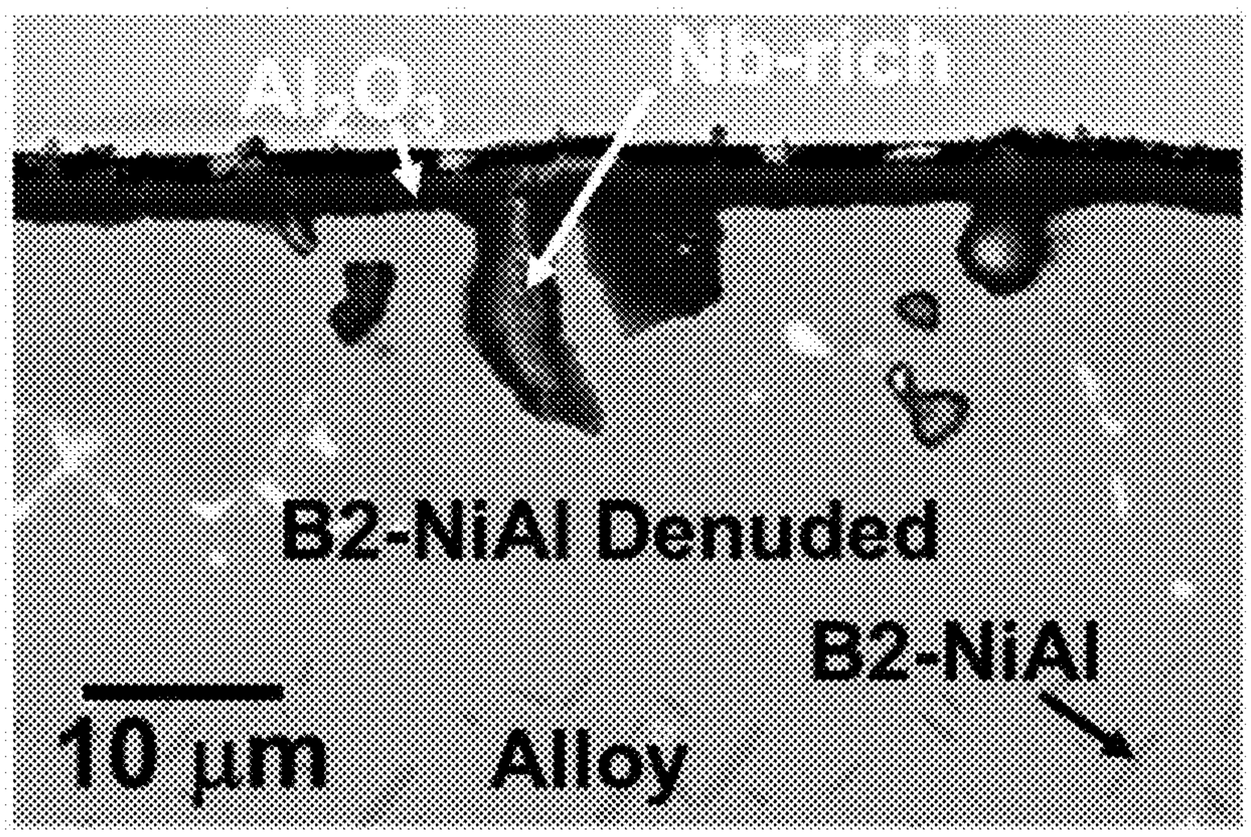
SEM
Al_2O_3
Nb-rich
B2-NiAl Denuded
B2-NiAl
10 μm
Alloy

FIG. 5

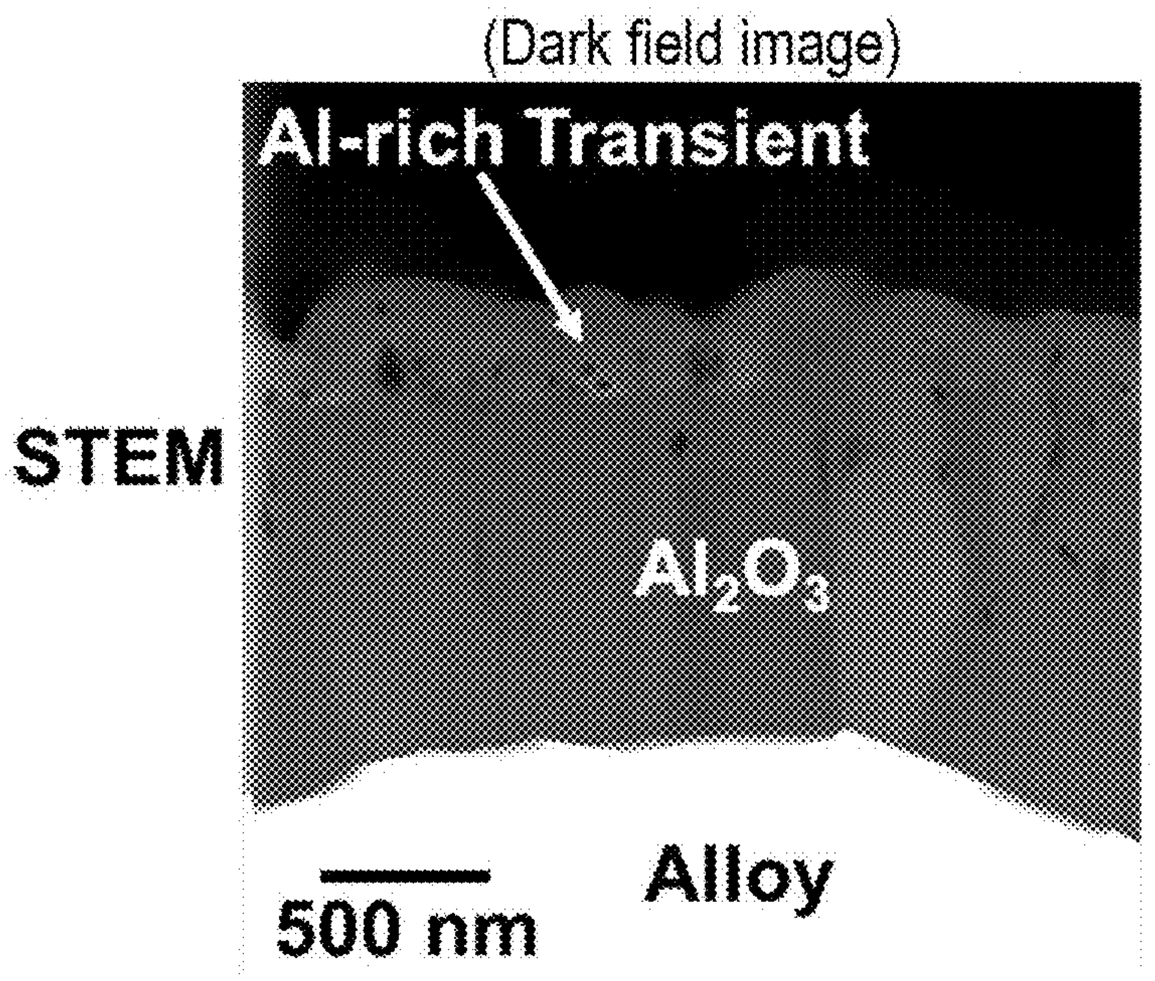
(Dark field image)
STEM
Al-rich Transient
Al_2O_3
500 nm
Alloy

FIG. 6

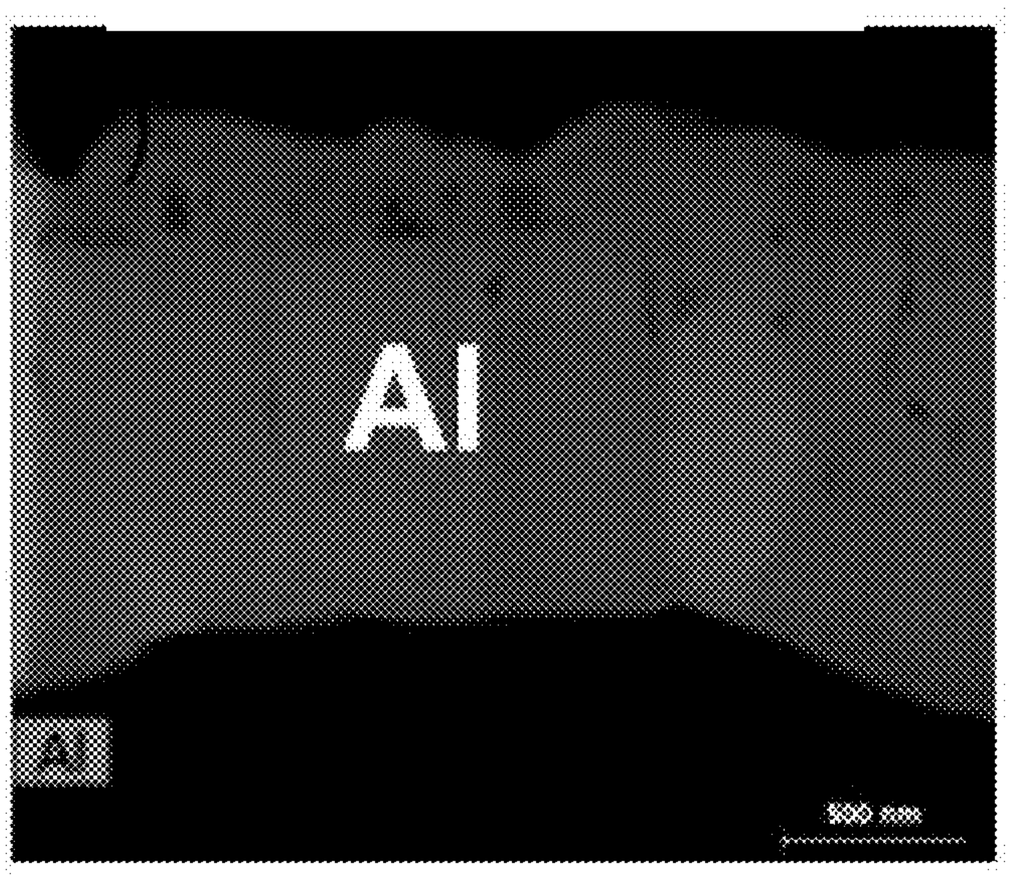

FIG. 7

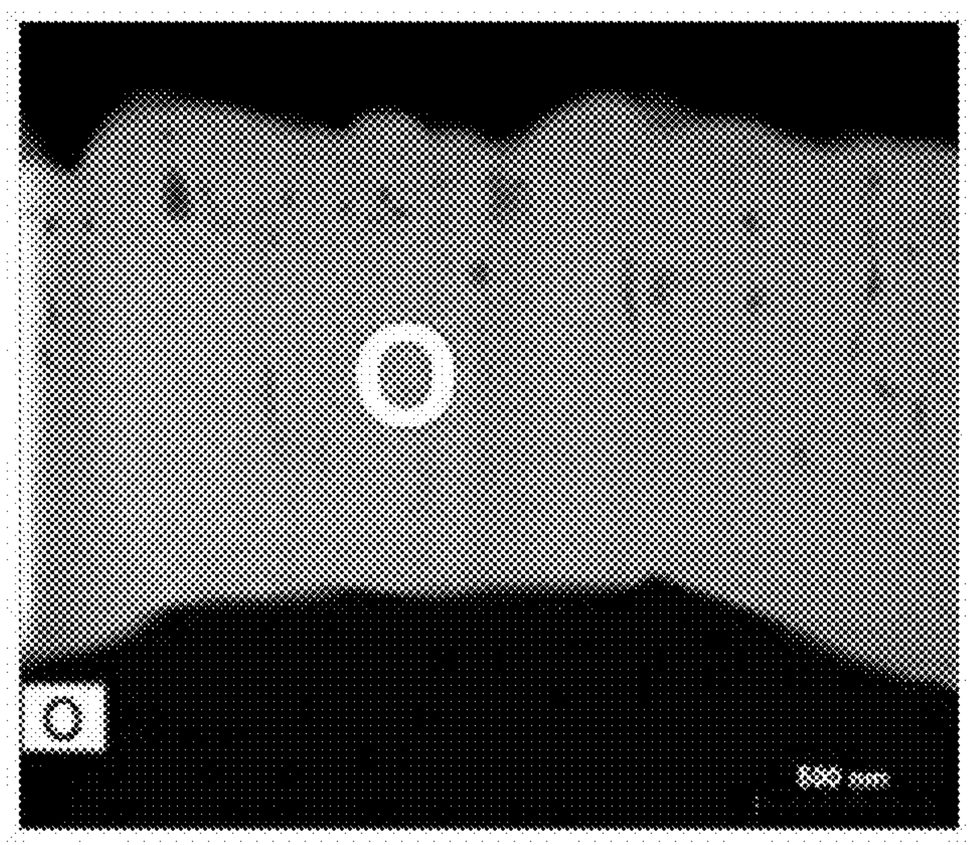

FIG. 8

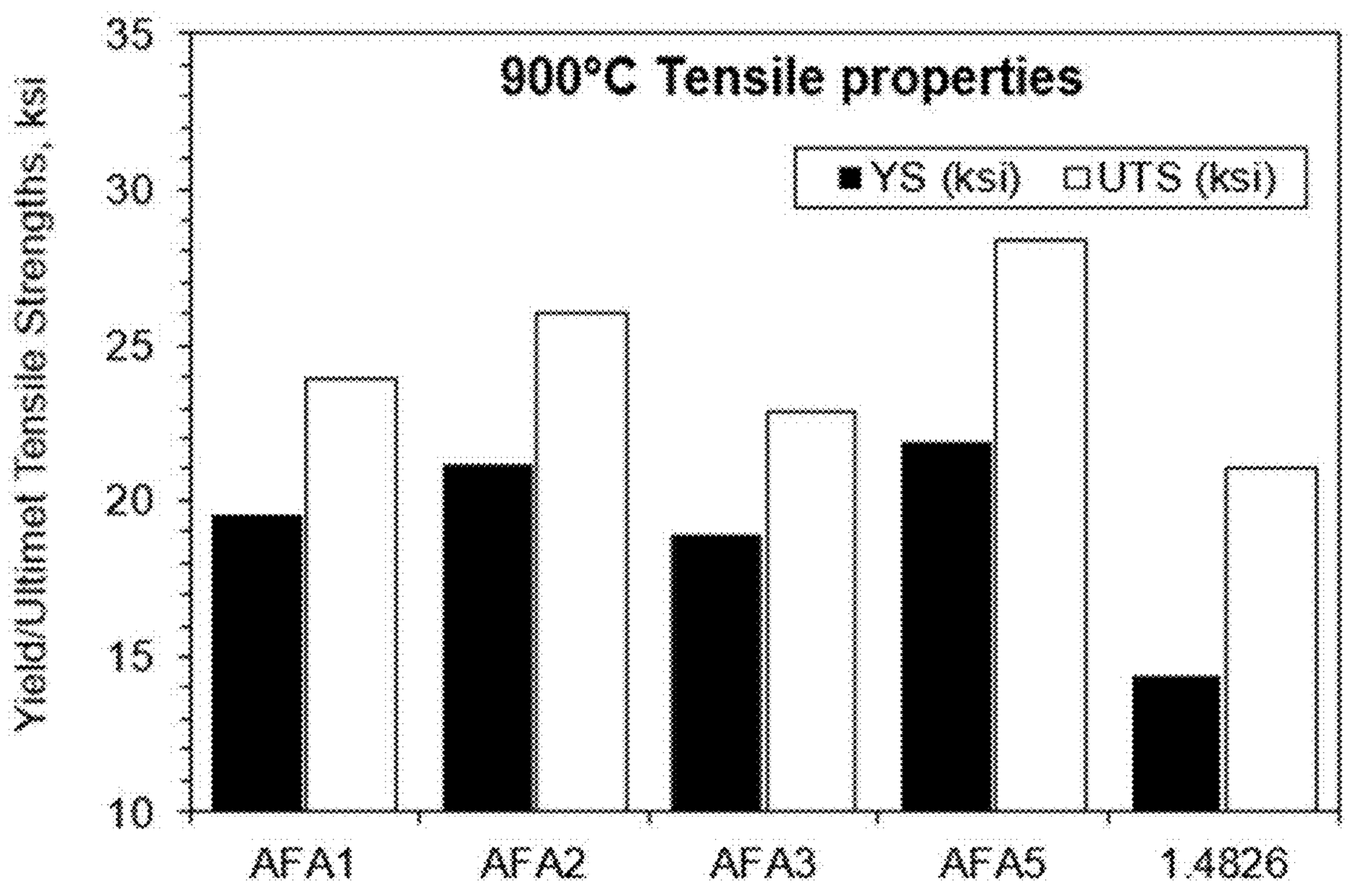
900°C Tensile properties
YS (ksi)
UTS (ksi)
Yield/Ultimet Tensile Strengths, ksi
35
30
25
20
15
10
AFA1
AFA2
AFA3
AFA5
1.4826

FIG. 9

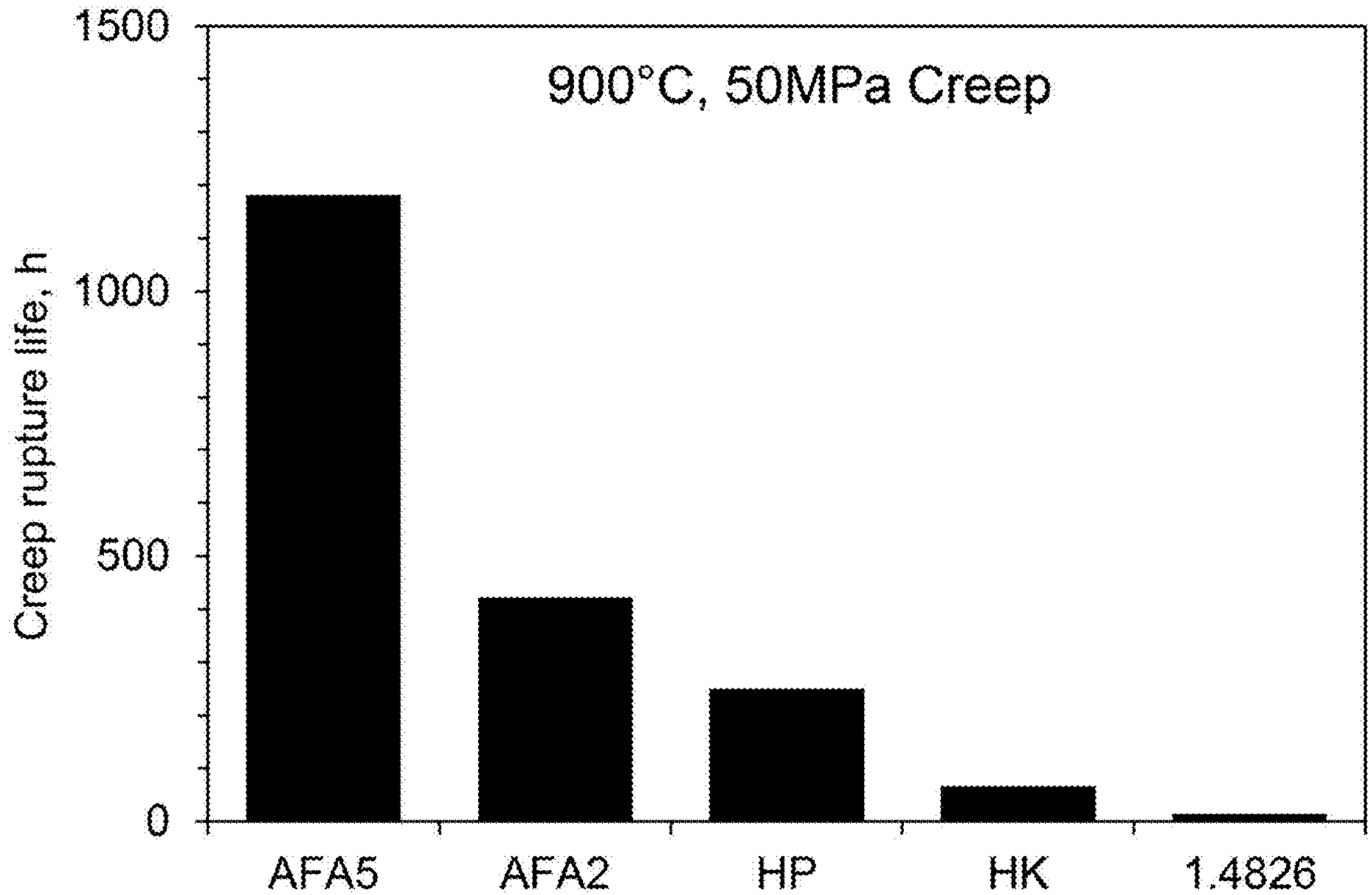
900°C, 50MPa Creep
Creep rupture life, h
1500
1000
500
0
AFA5
AFA2
HP
HK
1.4826

FIG. 10

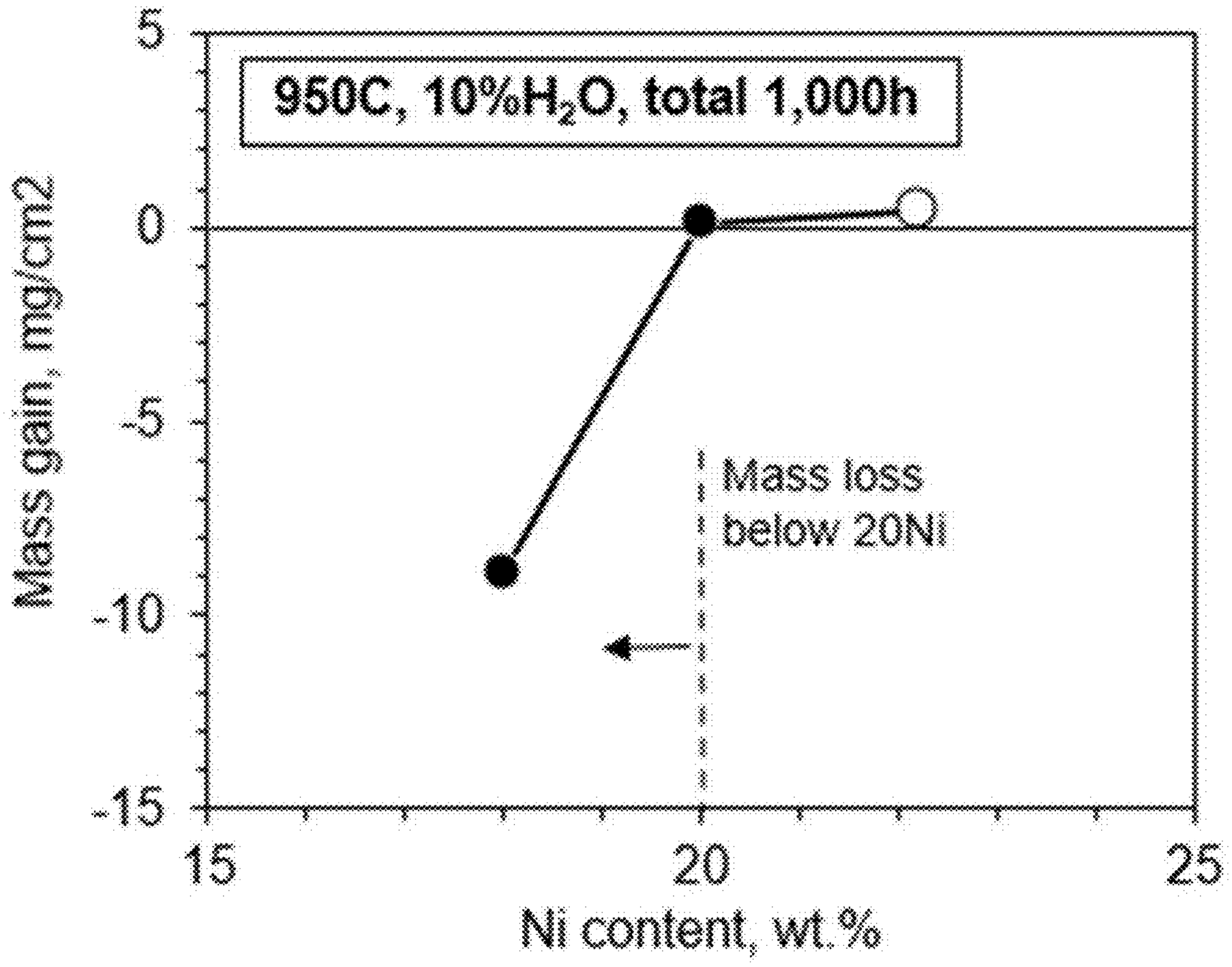
950C, 10%H2O, total 1,000h
Mass gain, mg/cm2
5
0
-5
-10
-15
Mass loss
below 20Ni
15
20
25
Ni content, wt.%

FIG. 11

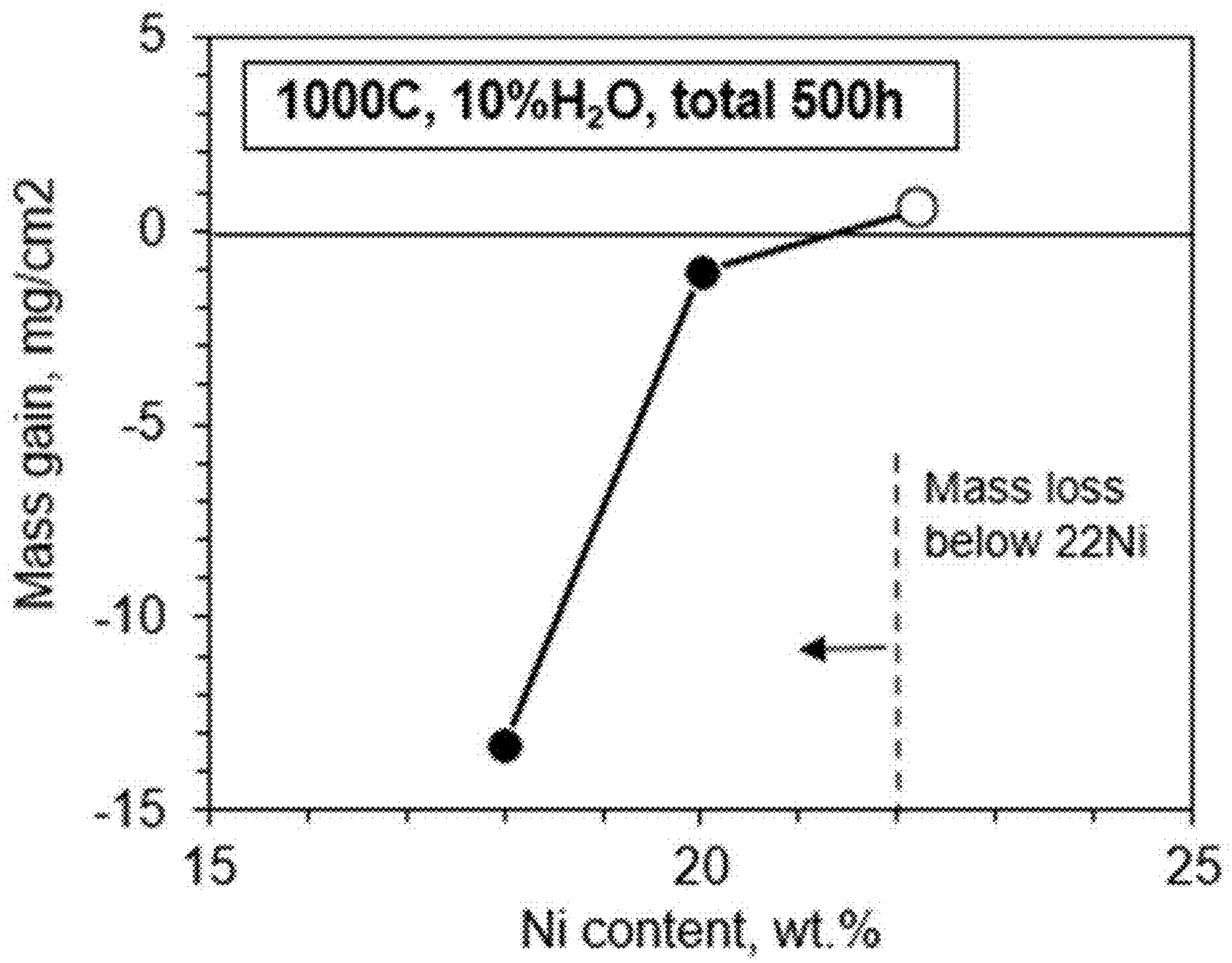
1000C, 10%H2O, total 500h
Mass gain, mg/cm2
5
0
-5
-10
-15
15
20
25
Mass loss
below 22Ni
Ni content, wt.%

FIG. 12

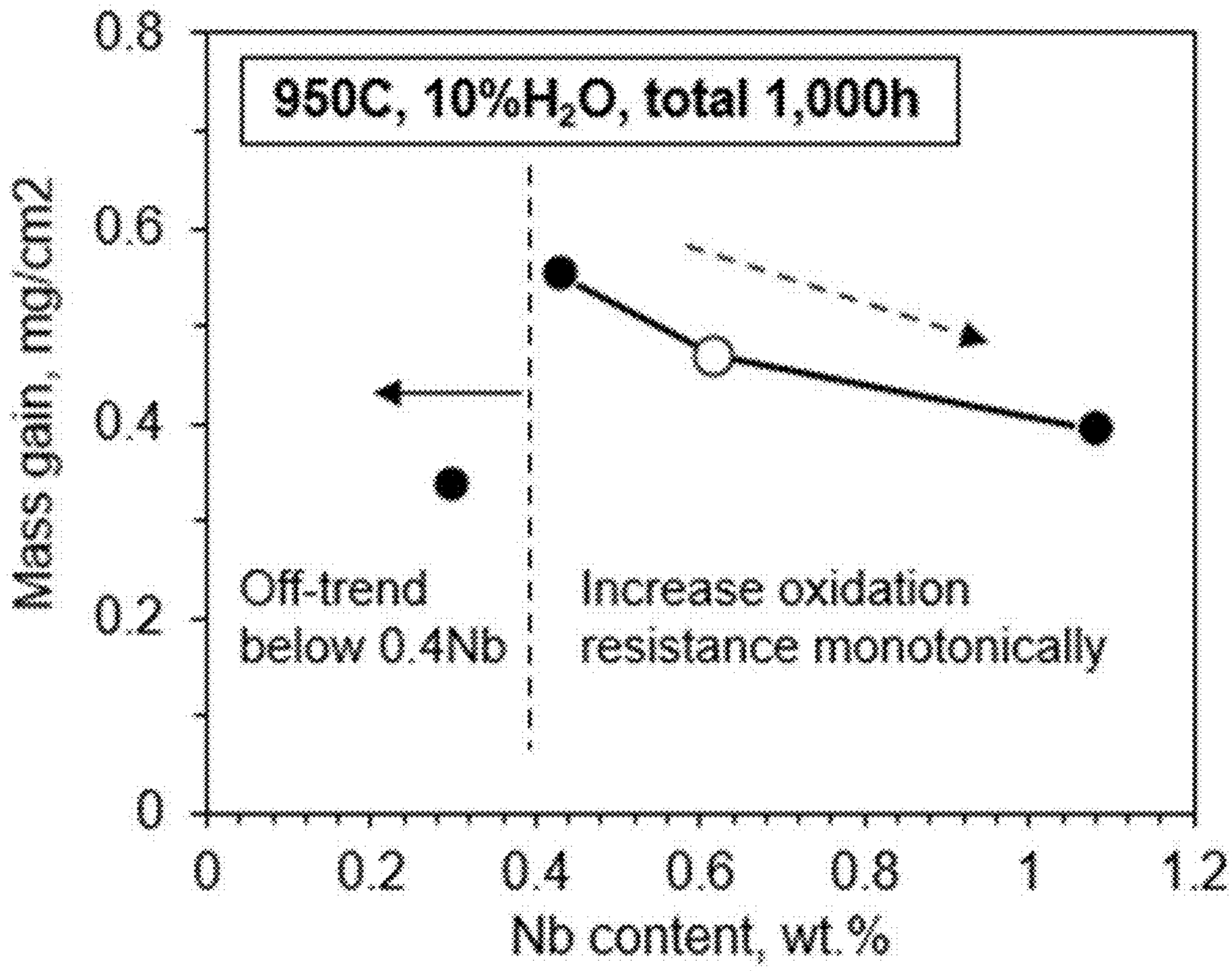
950C, 10%H2O, total 1,000h
Mass gain, mg/cm2
0
0.2
0.4
0.6
0.8
Off-trend
below 0.4Nb
Increase oxidation
resistance monotonically
0
0.2
0.4
0.6
0.8
1
1.2
Nb content, wt.%

FIG. 13

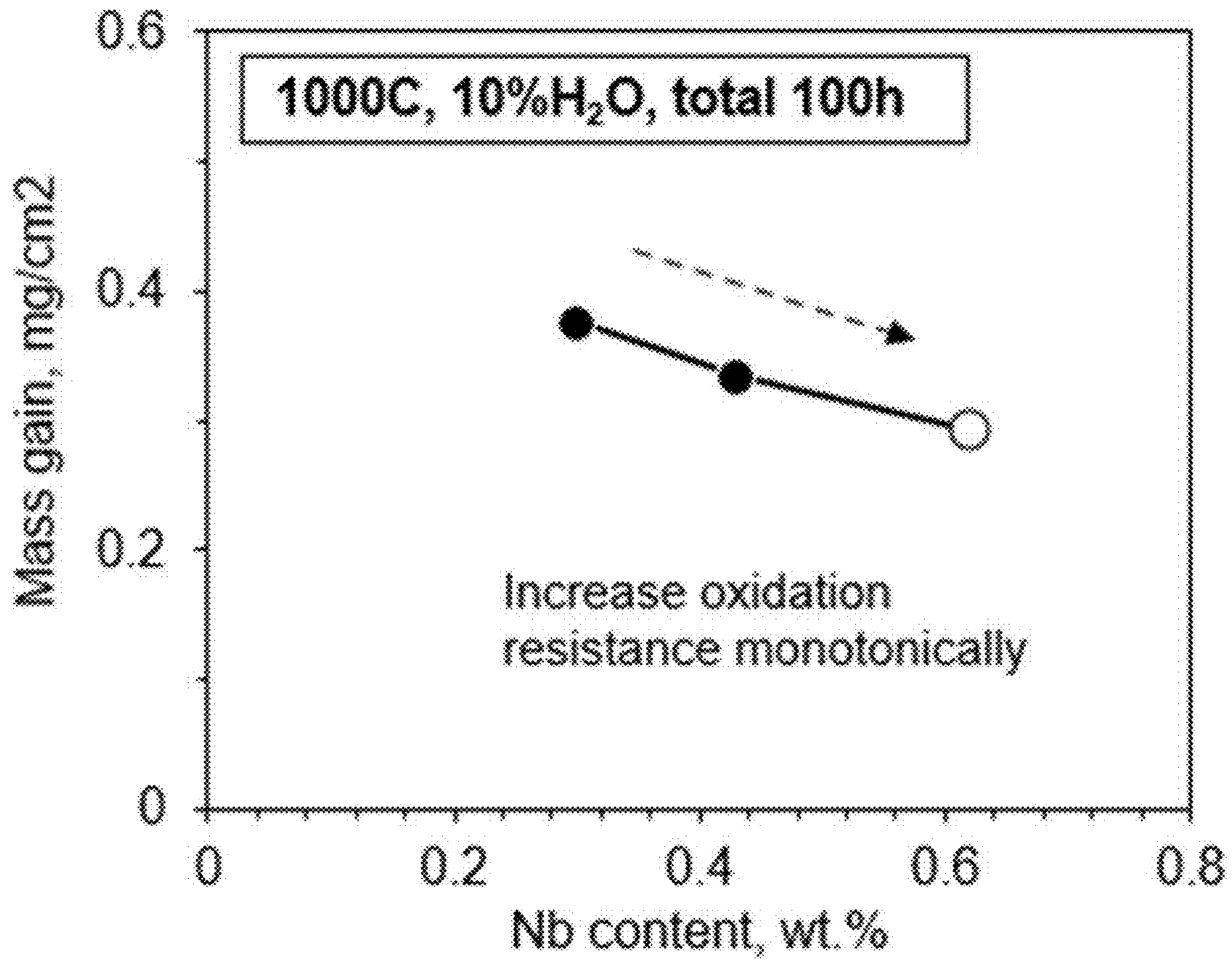
1000C, 10%H2O, total 100h
Mass gain, mg/cm2
0
0.2
0.4
0.6
0
0.2
0.4
0.6
0.8
Increase oxidation
resistance monotonically
Nb content, wt.%

FIG. 14

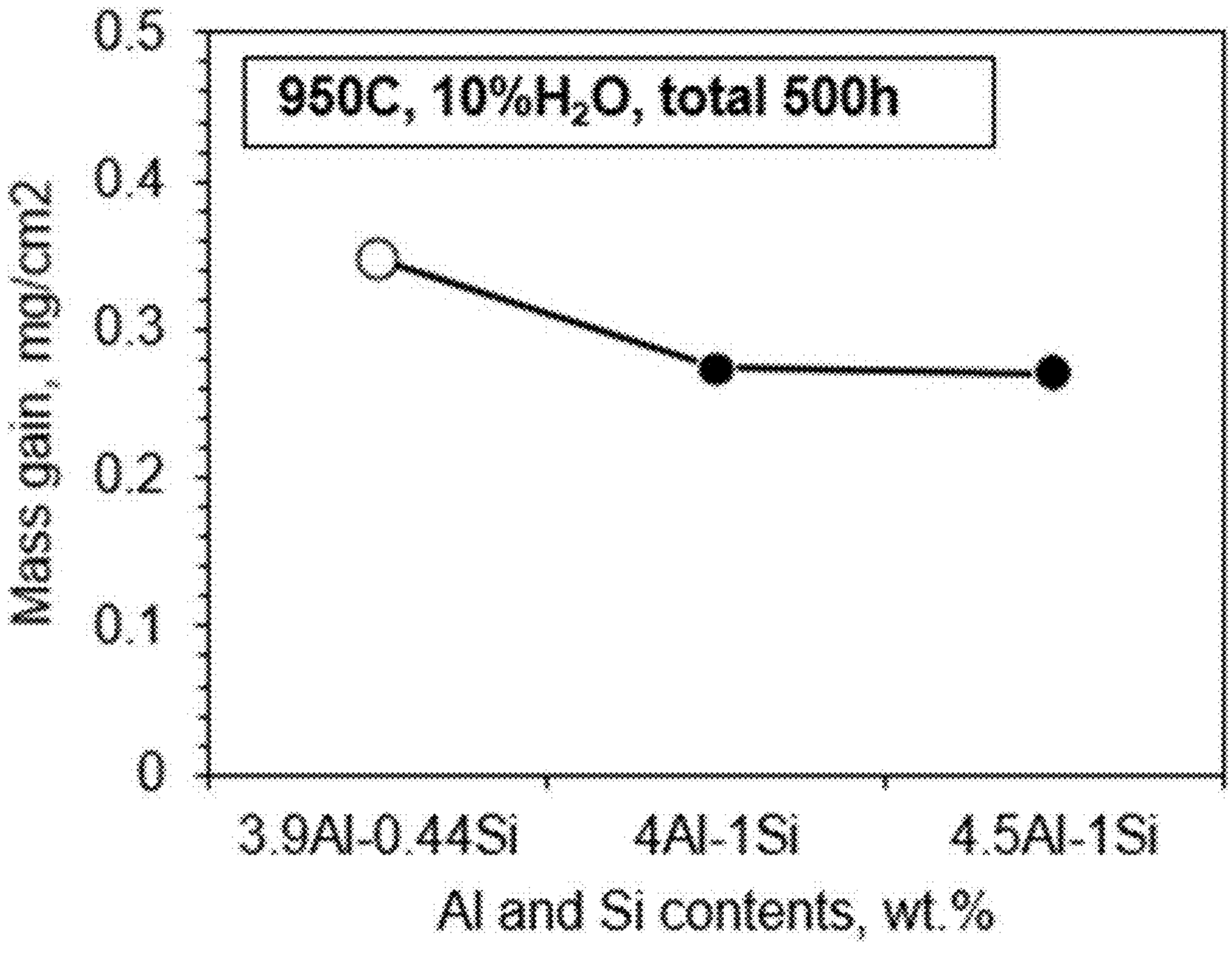
950C, 10%H2O, total 500h
Mass gain, mg/cm2
0.5
0.4
0.3
0.2
0.1
0
3.9Al-0.44Si
4Al-1Si
4.5Al-1Si
Al and Si contents, wt.%

FIG. 15

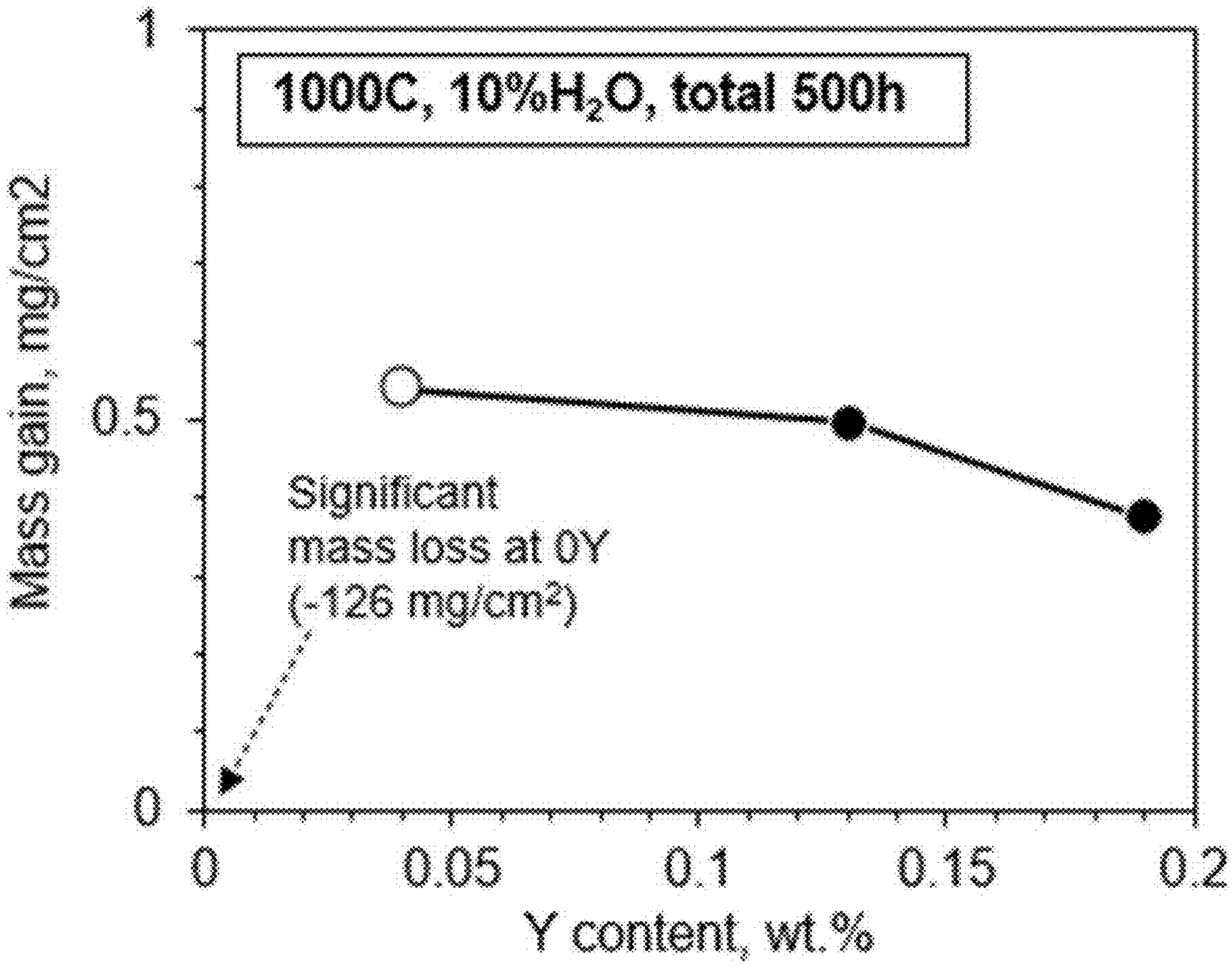
1
1000C, 10%H2O, total 500h
Mass gain, mg/cm2
0.5
0
Significant
mass loss at 0Y
(-126 mg/cm2)
0
0.05
0.1
0.15
0.2
Y content, wt.%

FIG. 16

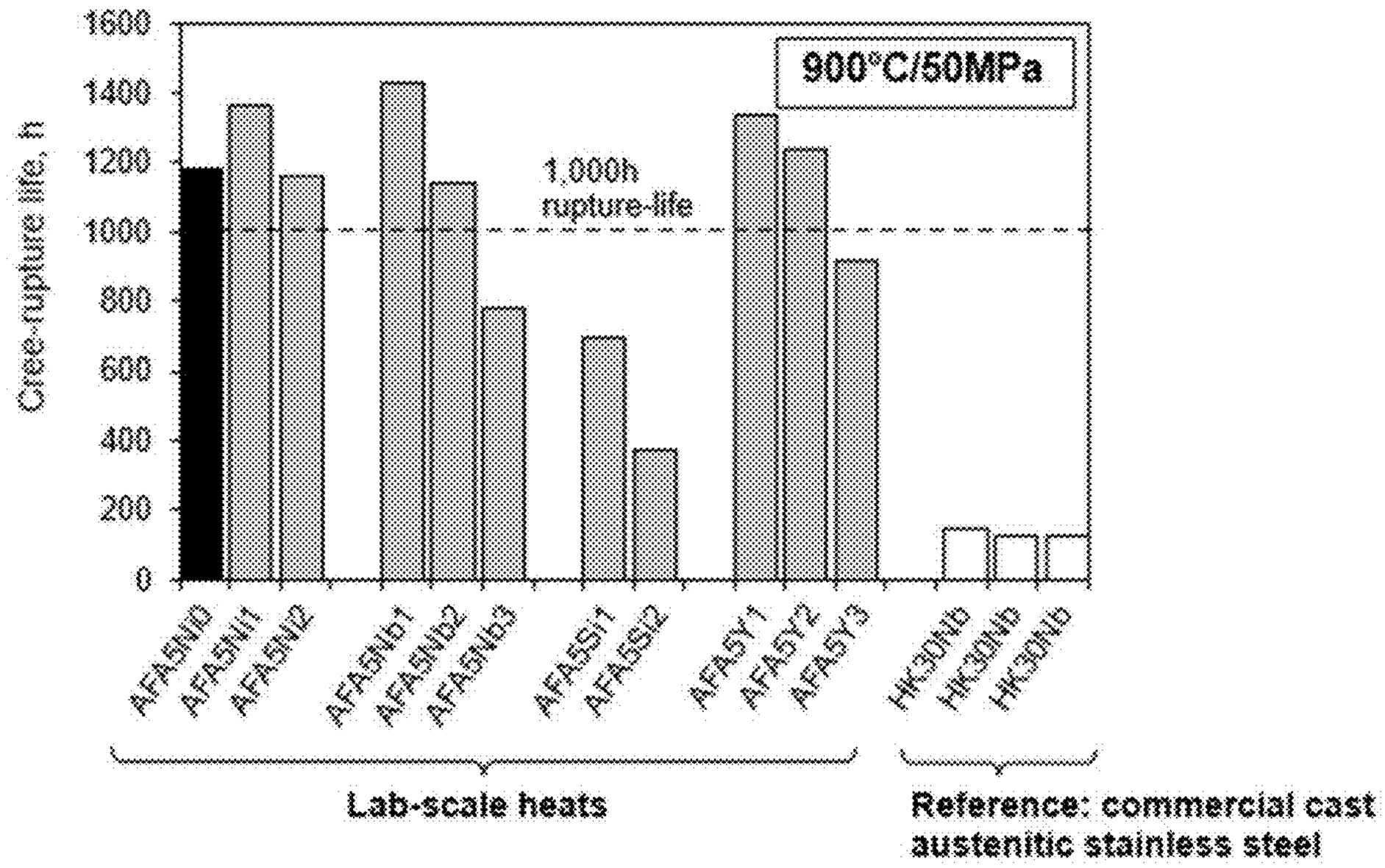
900°C/50MPa
1,000h rupture-life
Cree-rupture life, h
1600
1400
1200
1000
800
600
400
200
0
AFA5NI0
AFA5NI1
AFA5NI2
AFA5Nb1
AFA5Nb2
AFA5Nb3
AFA5Si1
AFA5Si2
AFA5Y1
AFA5Y2
AFA5Y3
HK30Nb
HK30Nb
HK30Nb
Lab-scale heats
Reference: commercial cast austenitic stainless steel

FIG. 17

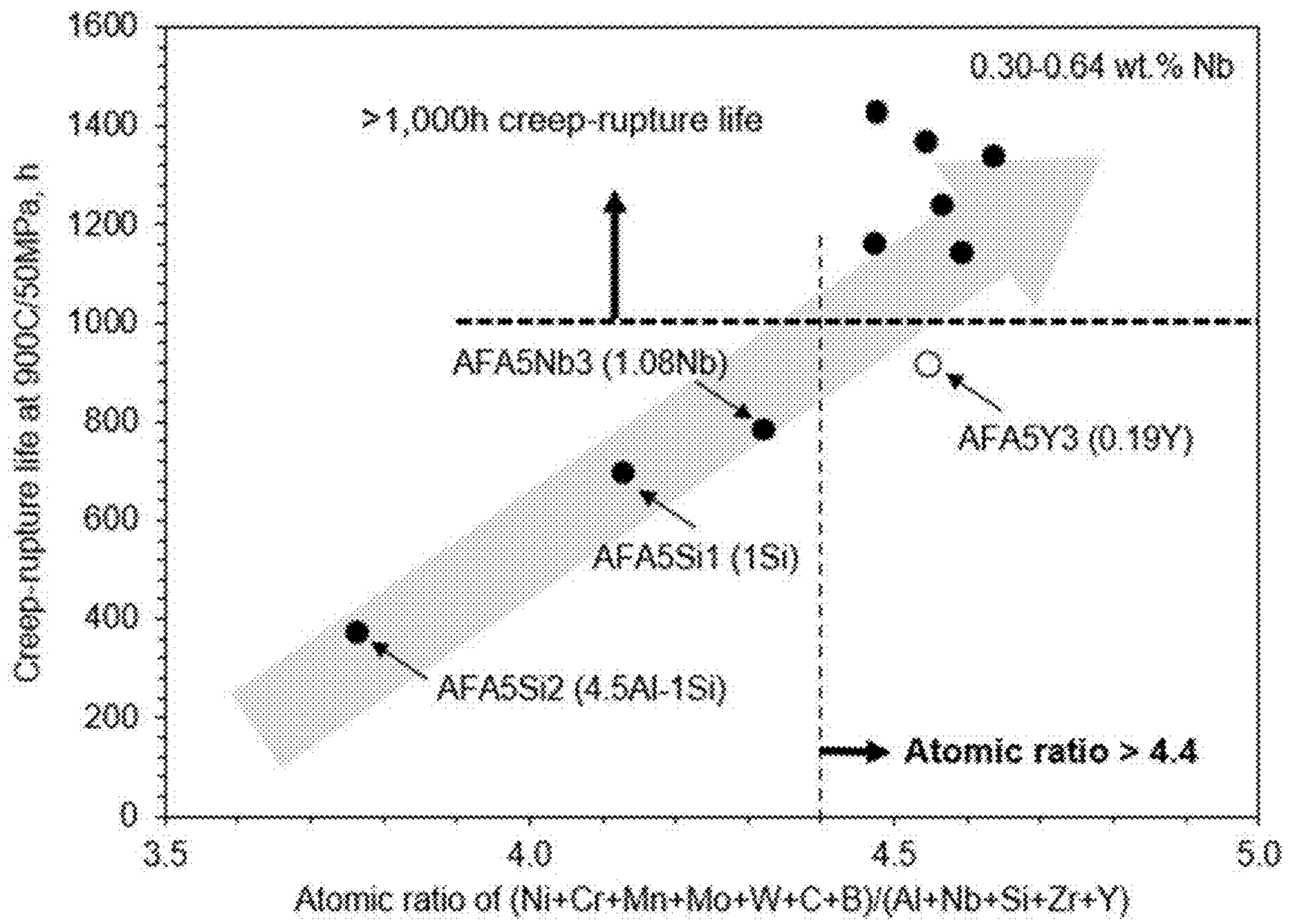
0.30-0.64 wt.% Nb
>1,000h creep-rupture life
AFA5Nb3 (1.08Nb)
AFA5Y3 (0.19Y)
AFA5Si1 (1Si)
AFA5Si2 (4.5Al-1Si)
Atomic ratio > 4.4
Creep-rupture life at 900C/50MPa, h
Atomic ratio of (Ni+Cr+Mn+Mo+W+C+B)/(Al+Nb+Si+Zr+Y)
1600
1400
1200
1000
800
600
400
200
0
3.5
4.0
4.5
5.0

FIG. 18

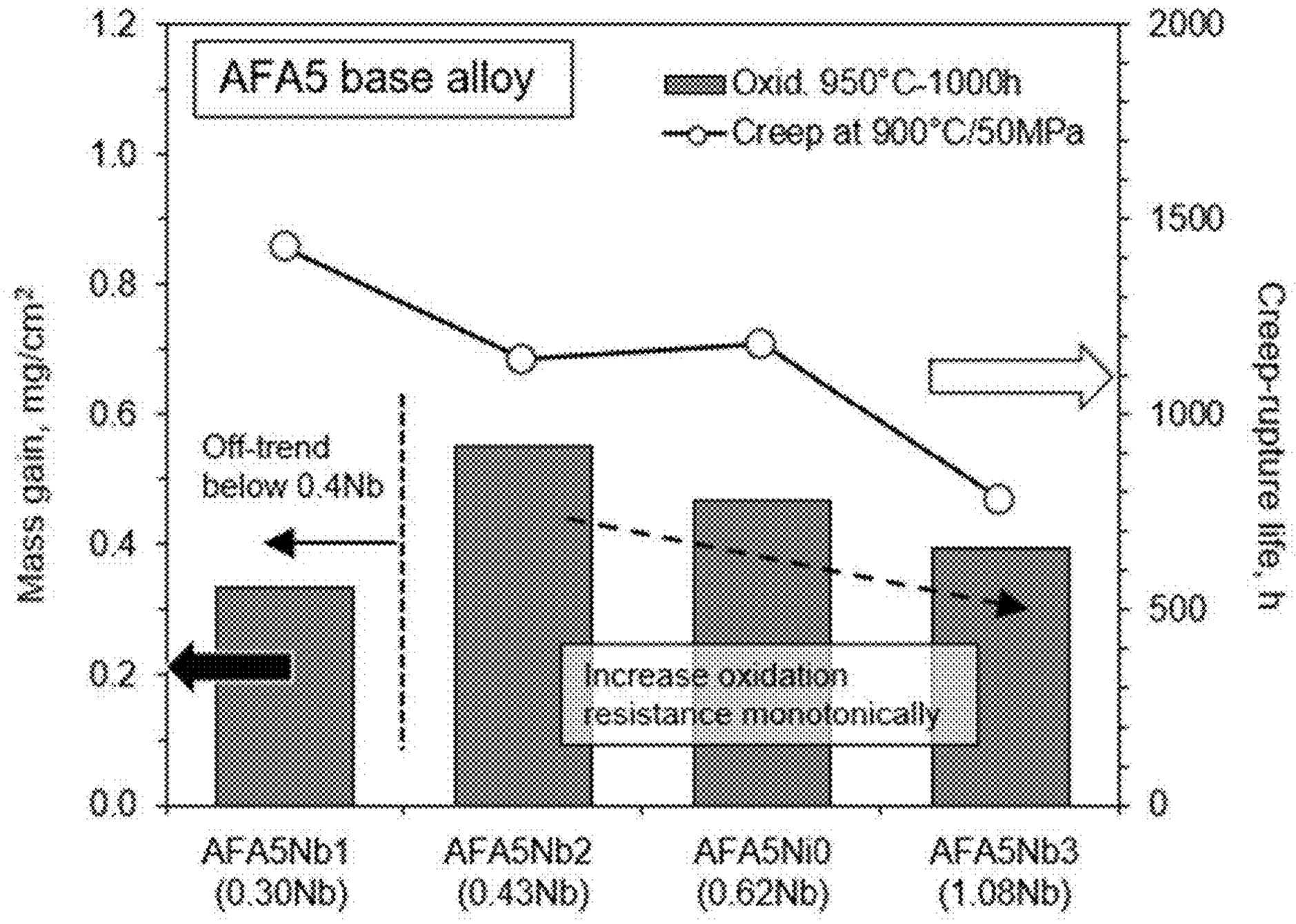
AFA5 base alloy
Oxid. 950°C-1000h
Creep at 900°C/50MPa
Mass gain, mg/cm²
Creep-rupture life, h
Off-trend
below 0.4Nb
Increase oxidation
resistance monotonically
0.0
0.2
0.4
0.6
0.8
1.0
1.2
0
500
1000
1500
2000
AFA5Nb1
(0.30Nb)
AFA5Nb2
(0.43Nb)
AFA5Nl0
(0.62Nb)
AFA5Nb3
(1.08Nb)

FIG. 19

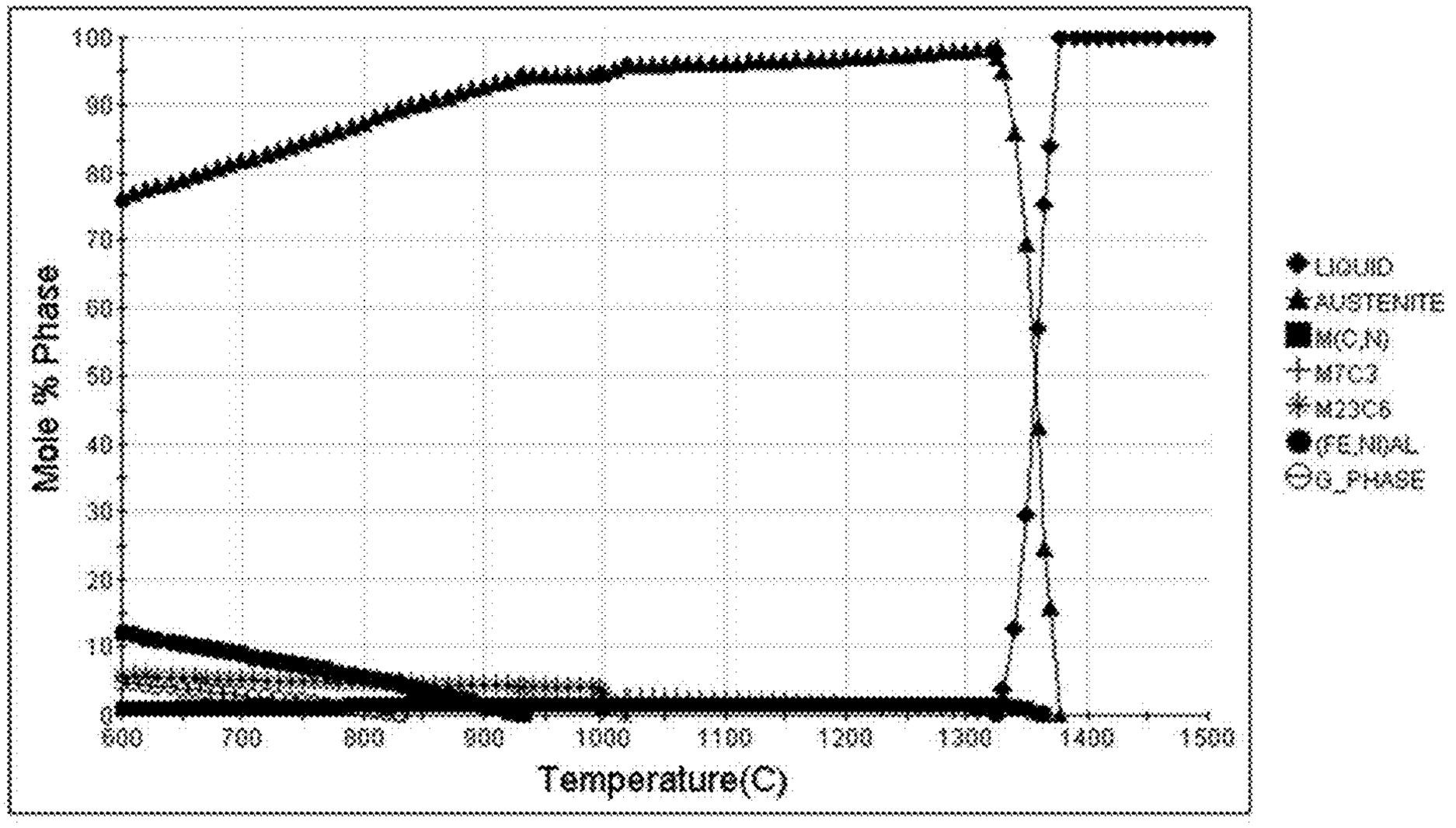
Mole % Phase
Temperature(C)
LIQUID
AUSTENITE
M(C,N)
M7C3
M23C6
(FE,NI)AL
G_PHASE

FIG. 20

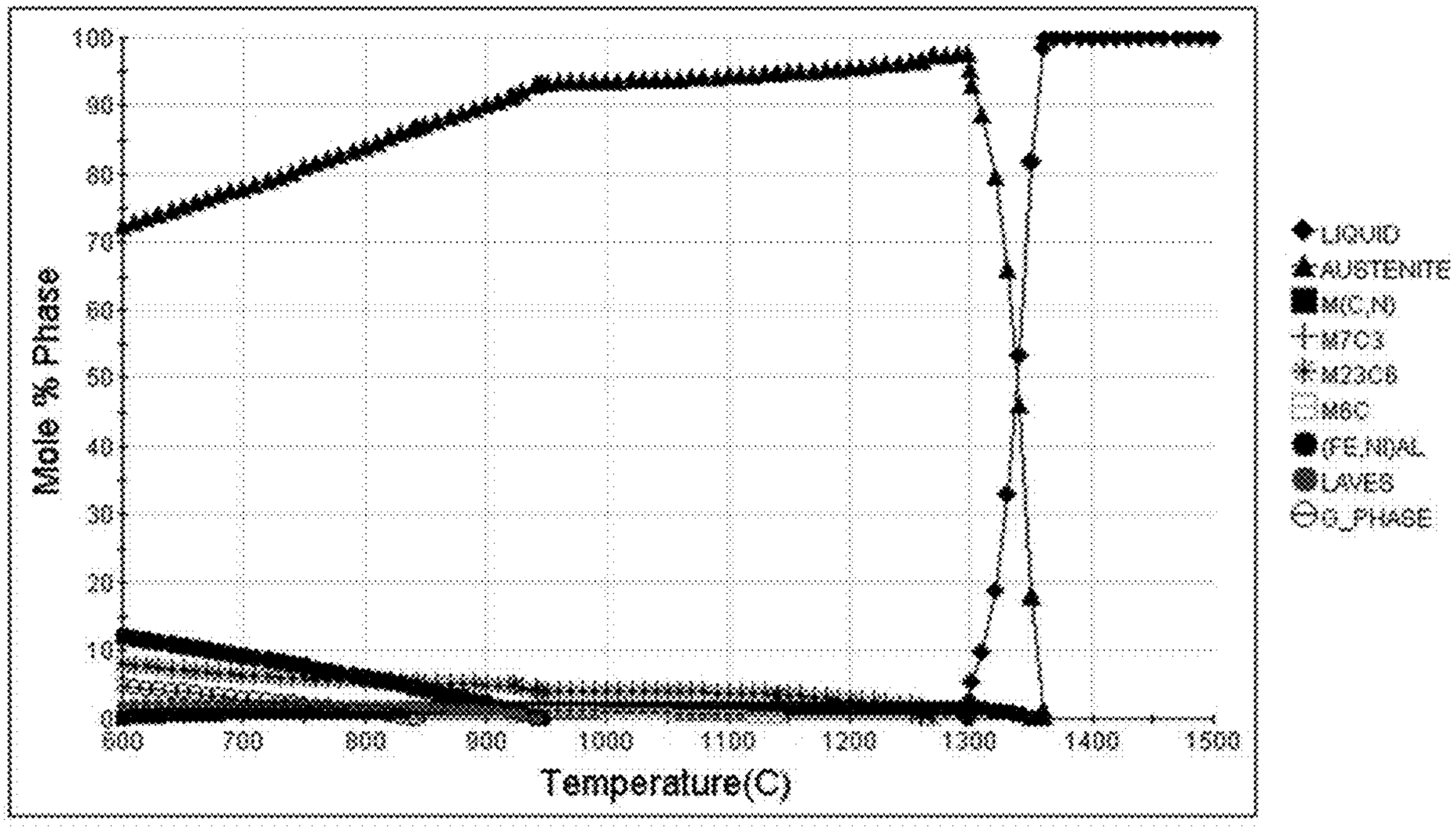
Mole % Phase
Temperature(C)
LIQUID
AUSTENITE
M(C,N)
M7C3
M23C6
M6C
(FE,NI)AL
LAVES
σ_PHASE

FIG. 21

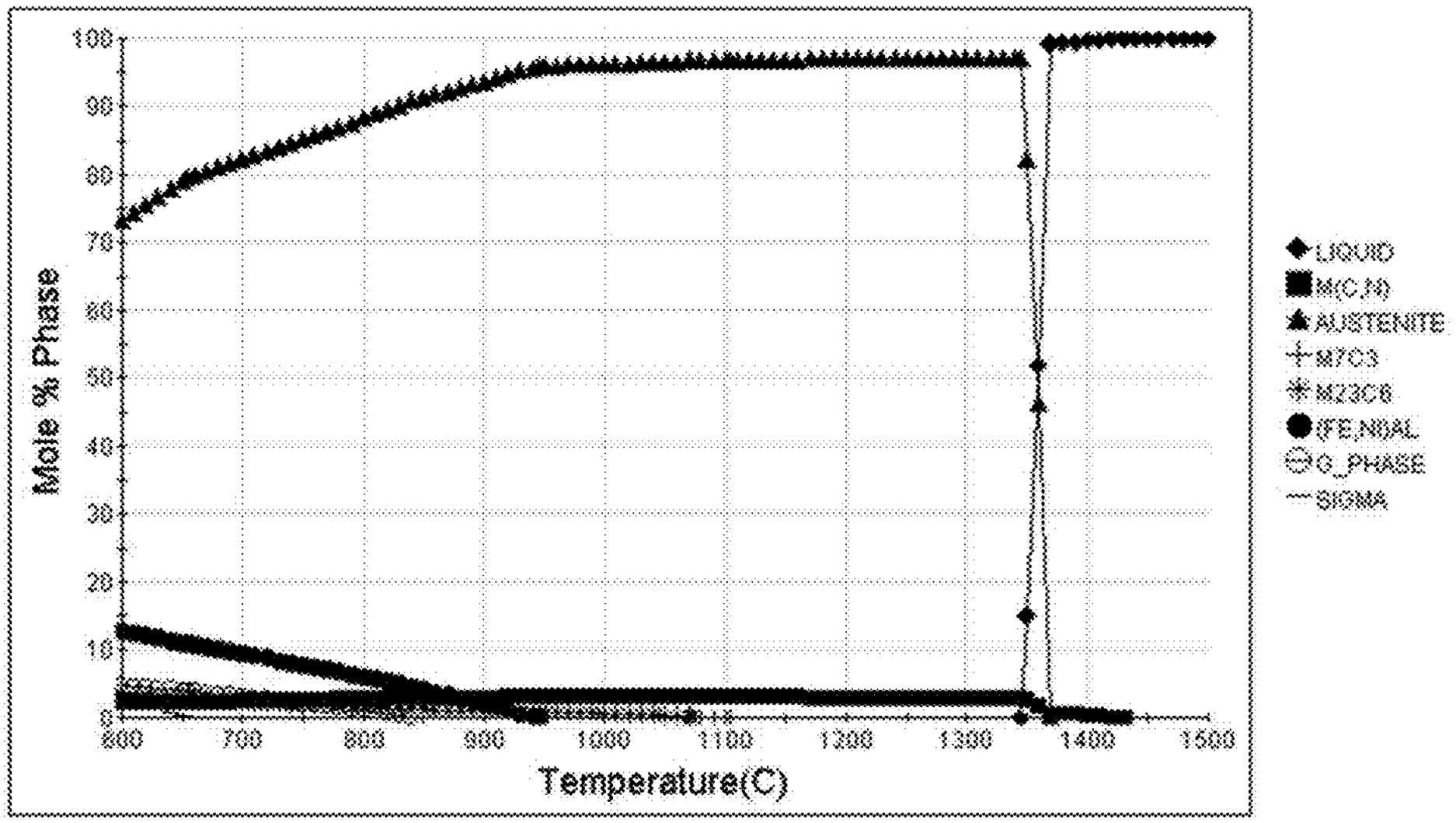
Mole % Phase
100
90
80
70
60
50
40
30
20
10
0
600
700
800
900
1000
1100
1200
1300
1400
1500
Temperature(C)
LIQUID
M(C,N)
AUSTENITE
M7C3
M23C6
(FE,NB)AL
G_PHASE
SIGMA

FIG. 22

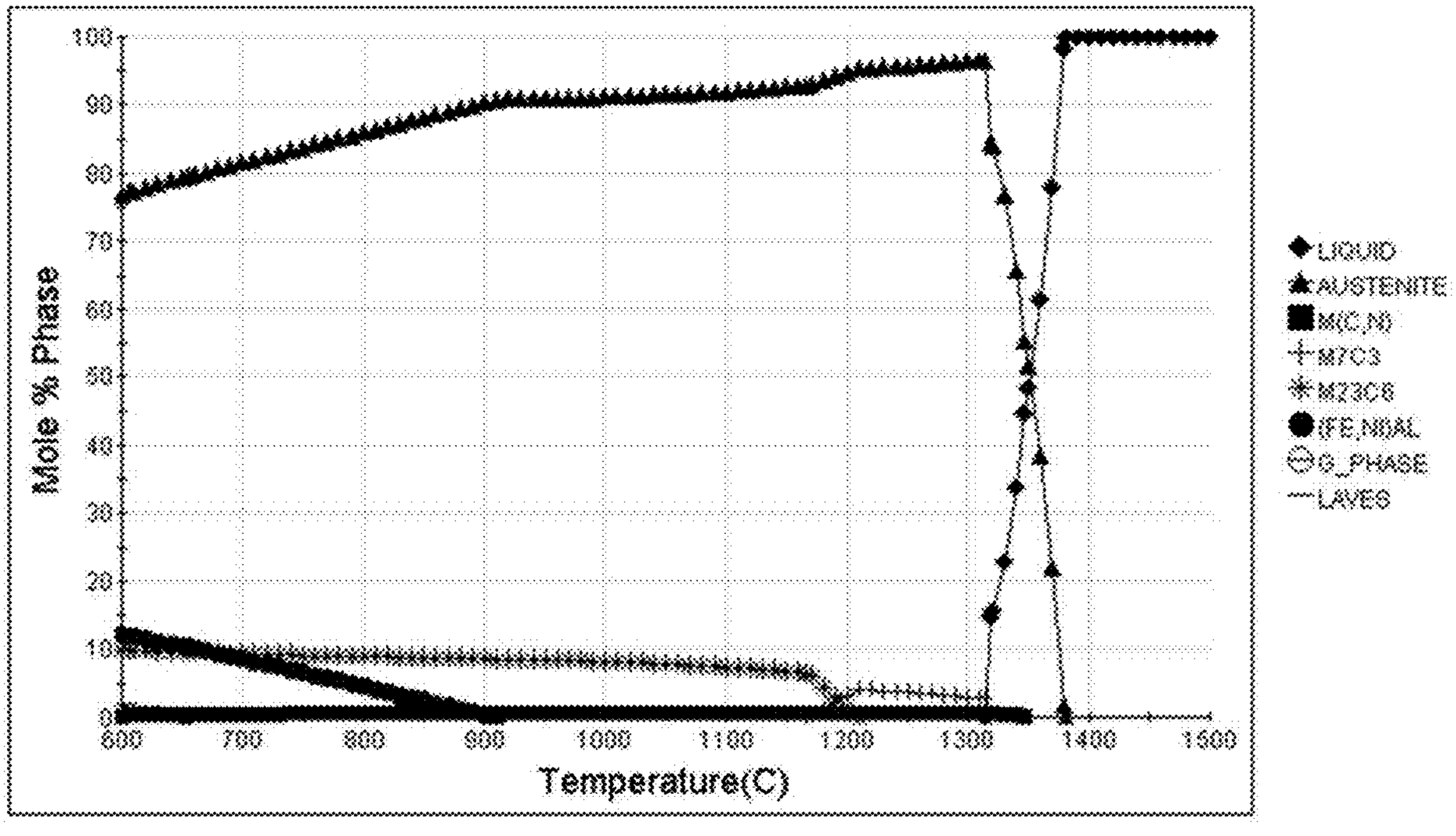
Mole % Phase
Temperature(C)
LIQUID
AUSTENITE
M(C,N)
M7C3
M23C6
IFE_NBAL
G_PHASE
LAVES

FIG. 23

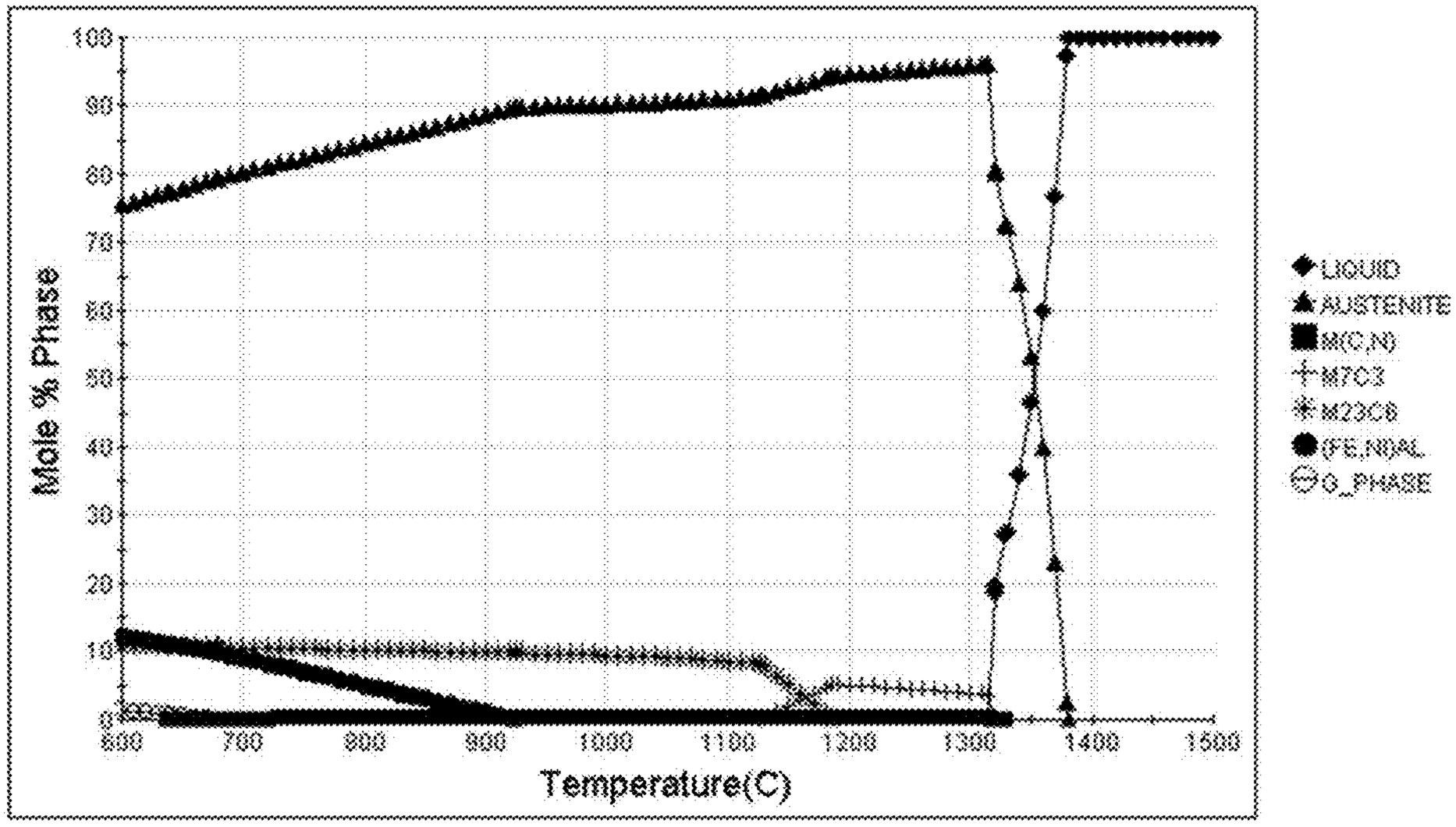
Mole % Phase
100
90
80
70
60
50
40
30
20
10
0
600
700
800
900
1000
1100
1200
1300
1400
1500
Temperature(C)
LIQUID
AUSTENITE
M(C,N)
M7C3
M23C6
(FE,NI)AL
G_PHASE

FIG. 24

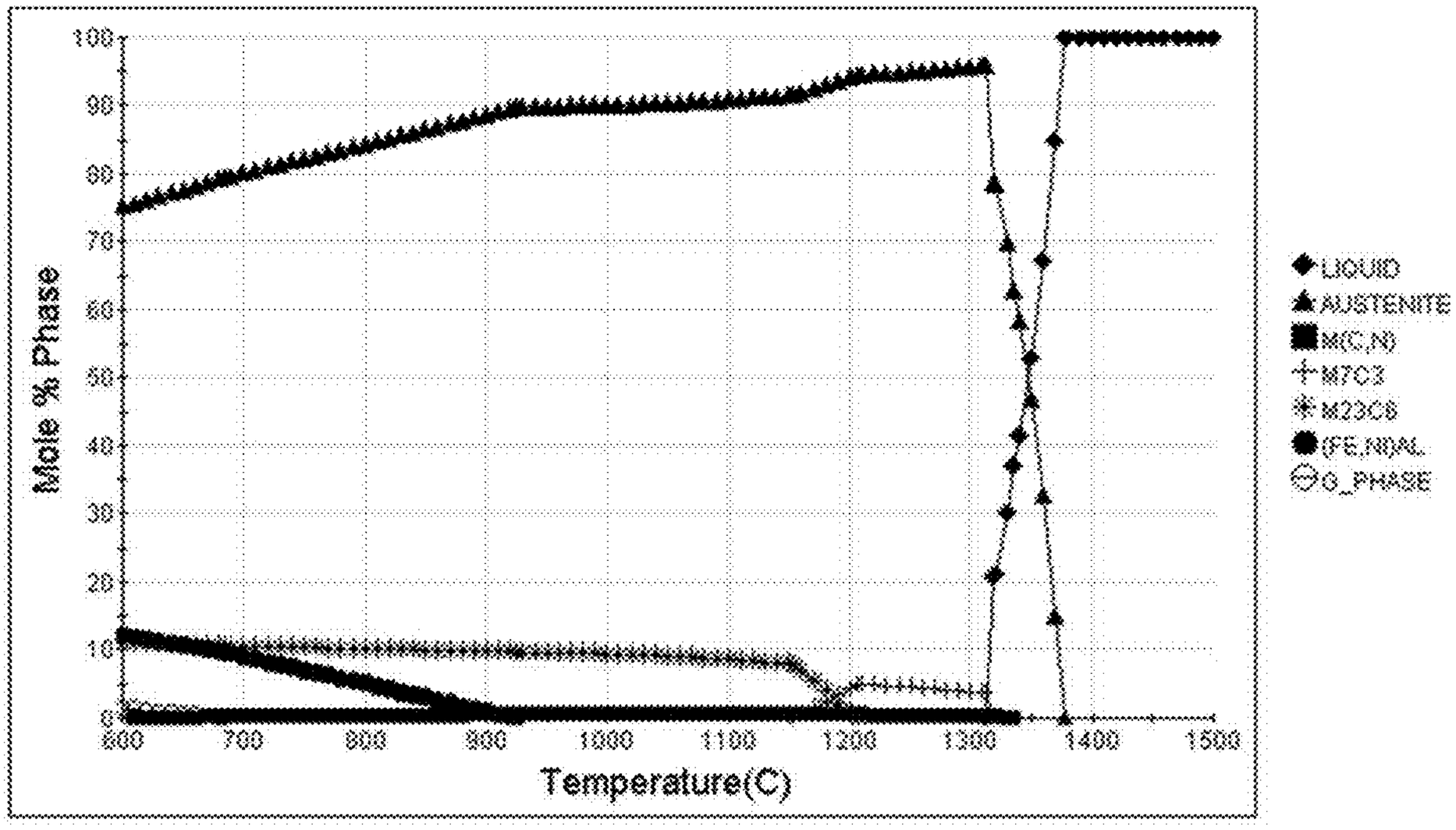
Mole % Phase
Temperature(C)
LIQUID
AUSTENITE
M(C,N)
M7C3
M23C6
(FE,NB)AL
G_PHASE

FIG. 25

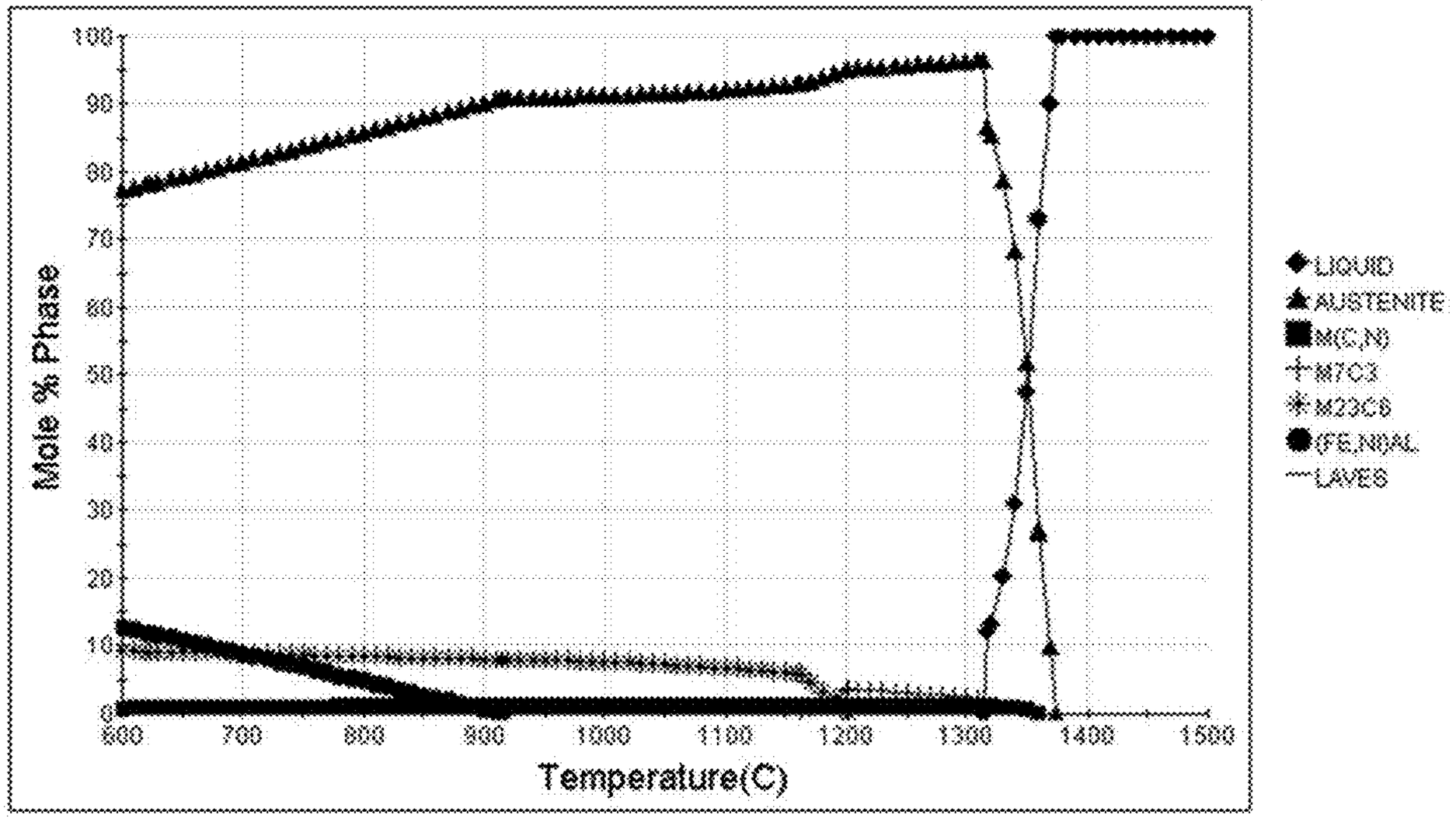
Mole % Phase
100
90
80
70
60
50
40
30
20
10
0
600
700
800
900
1000
1100
1200
1300
1400
1500
Temperature(C)
LIQUID
AUSTENITE
M(C,N)
M7C3
M23C6
(FE,NI)AL
LAVES

FIG. 26

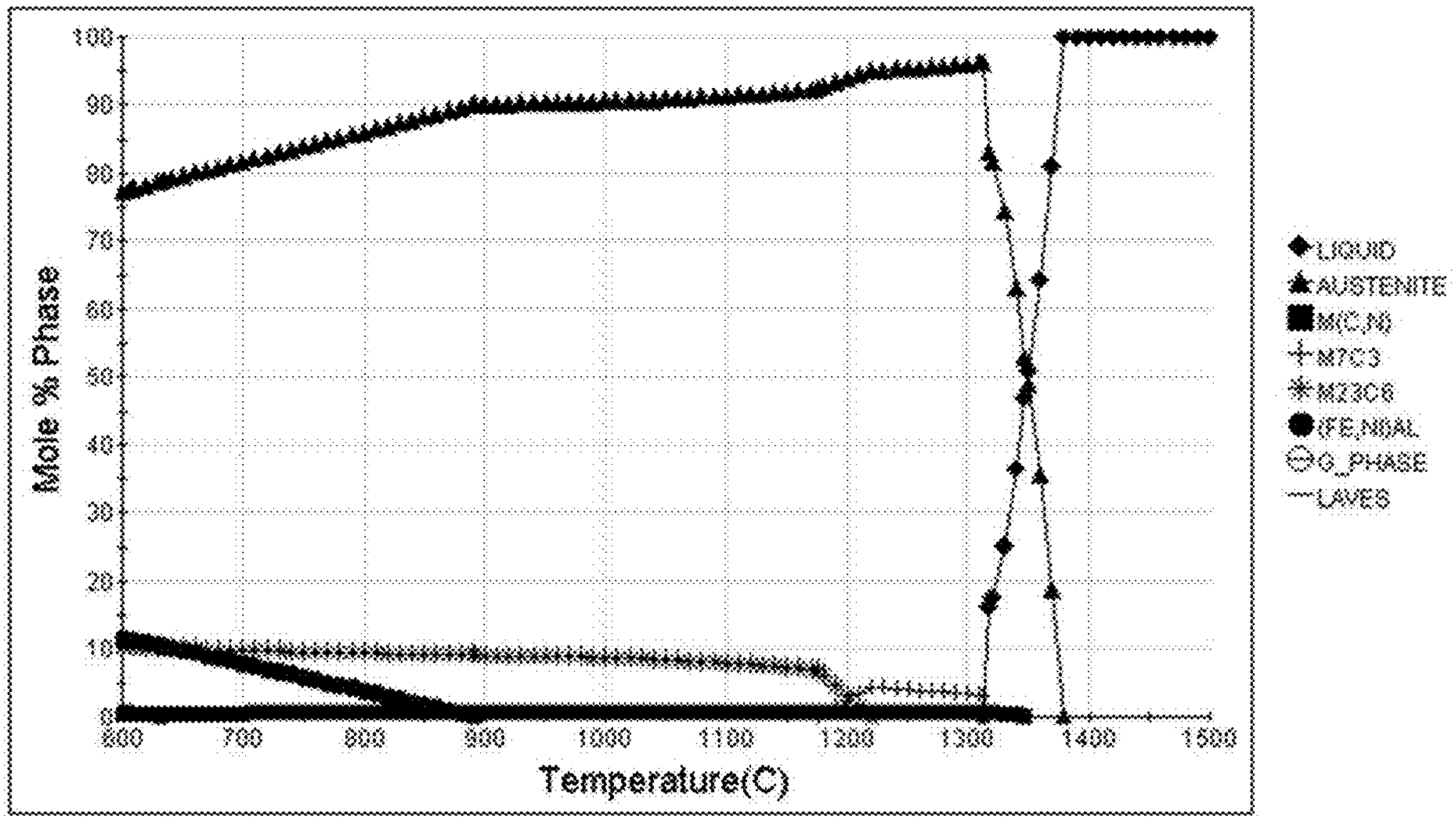
Mole % Phase
Temperature(C)
100
90
80
70
60
50
40
30
20
10
0
600
700
800
900
1000
1100
1200
1300
1400
1500
LIQUID
AUSTENITE
M(C,N)
M7C3
M23C6
(FE,NB)AL
G_PHASE
LAVES

FIG. 27

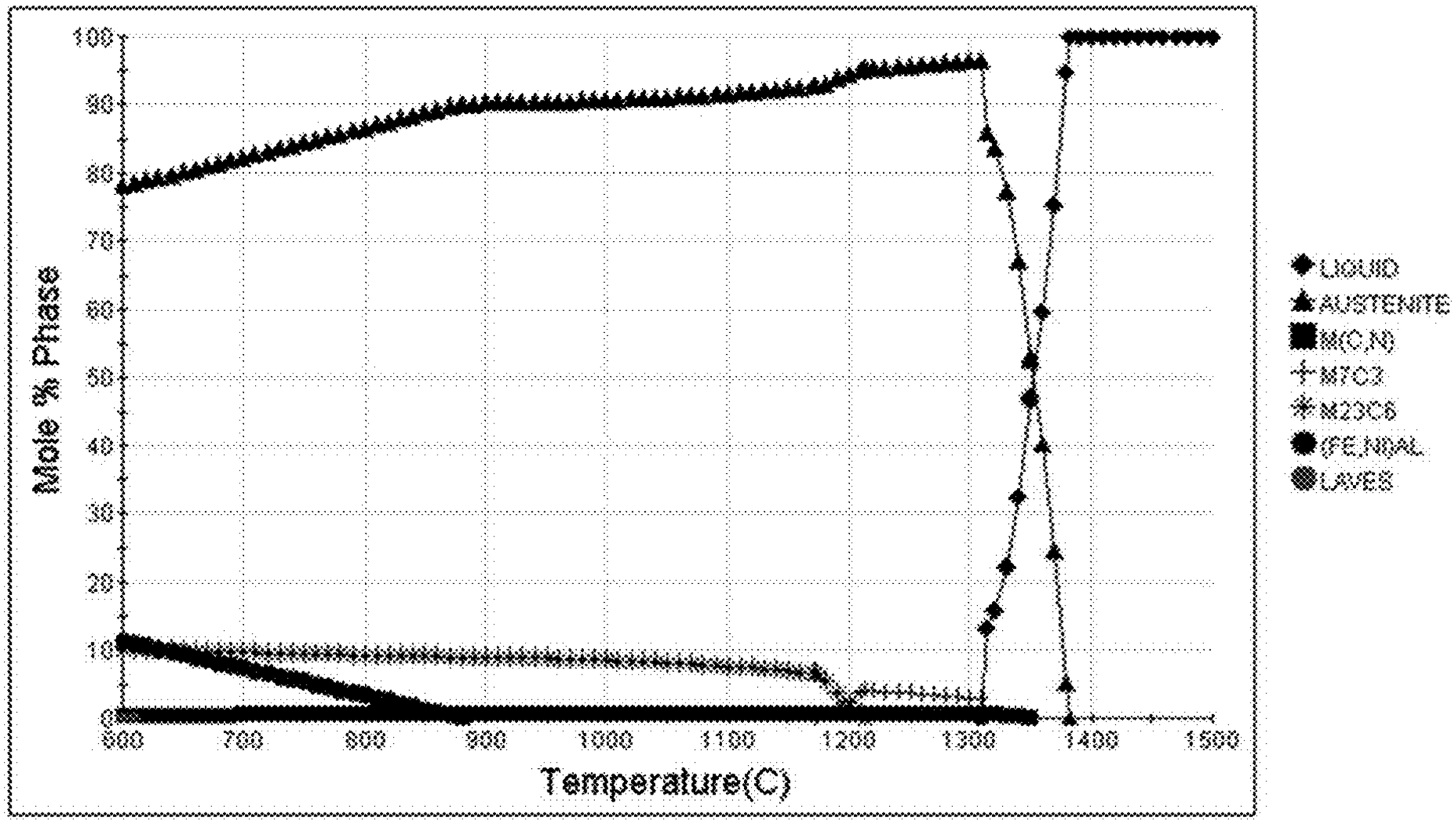
Mole % Phase
100
90
80
70
60
50
40
30
20
10
0
600
700
800
900
1000
1100
1200
1300
1400
1500
Temperature(C)
LIQUID
AUSTENITE
M(C,N)
M7C3
M23C6
(FE,NB)AL
LAVES

FIG. 28

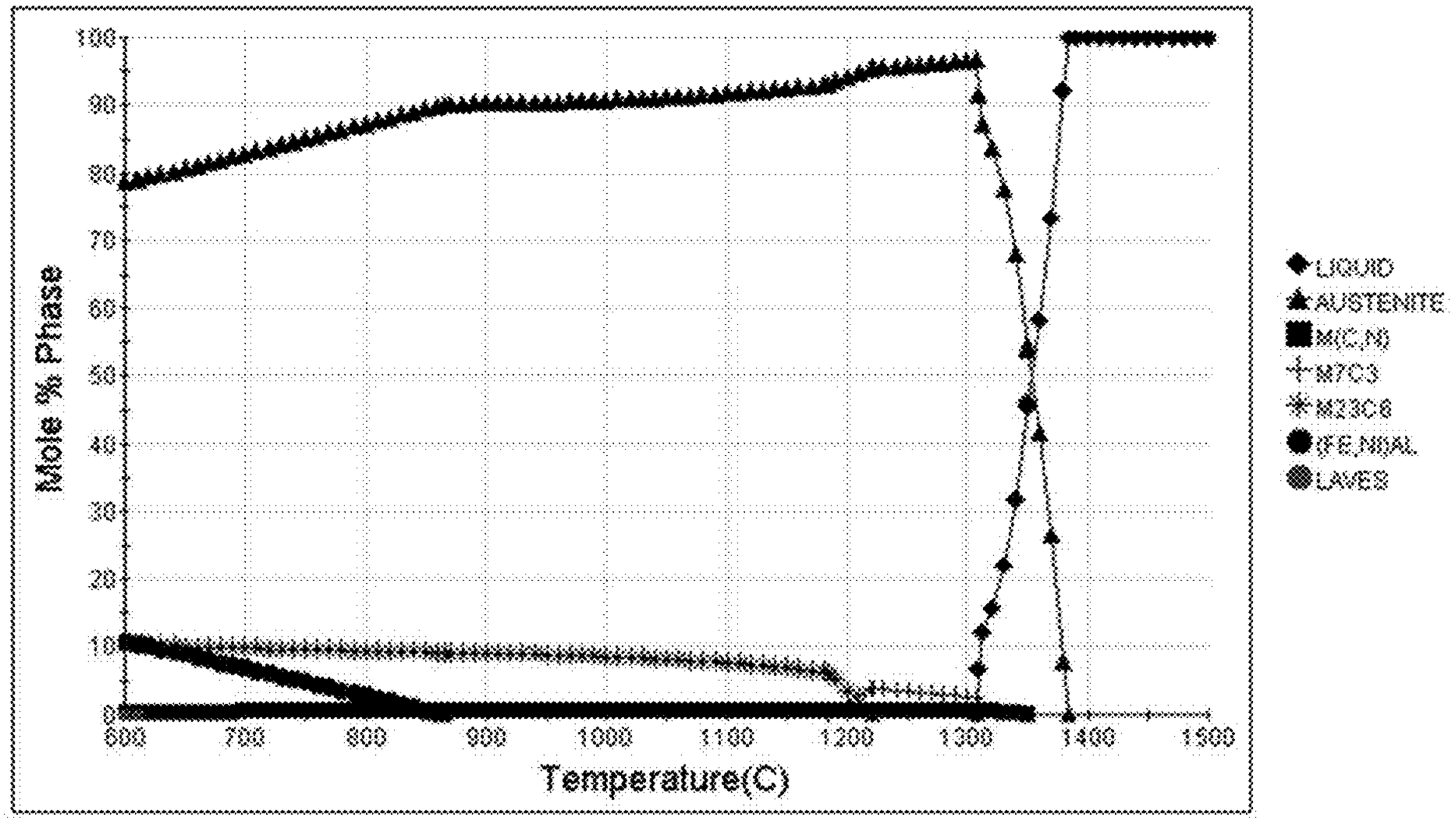
Mole % Phase
100
90
80
70
60
50
40
30
20
10
0
600
700
800
900
1000
1100
1200
1300
1400
1500
Temperature(C)
LIQUID
AUSTENITE
M(C,N)
M7C3
M23C6
(FE,NI)AL
LAVES

FIG. 29

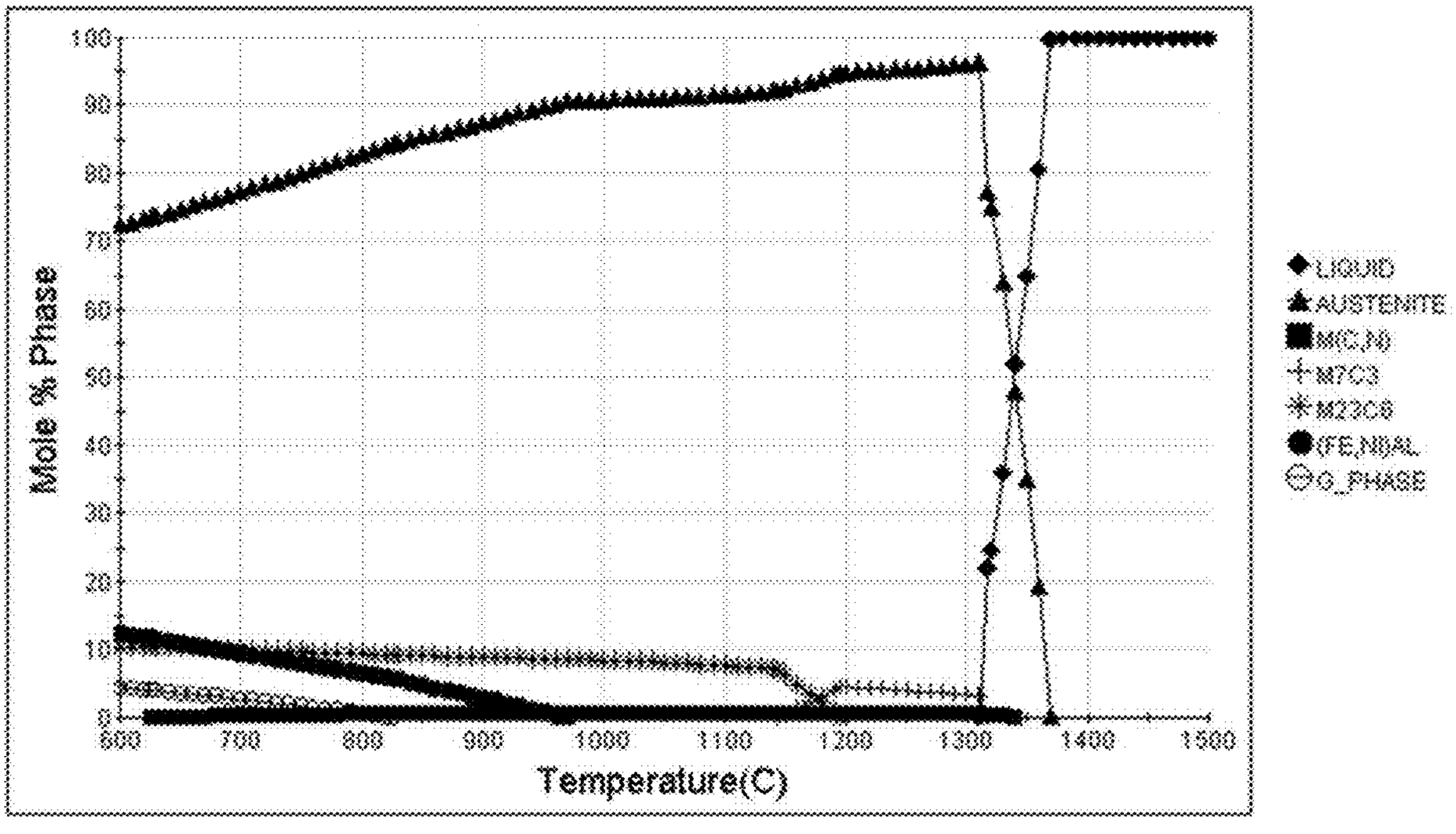
Mole % Phase
Temperature(C)
LIQUID
AUSTENITE
M(C,N)
M7C3
M23C6
(FE,NB)AL
G_PHASE

FIG. 30

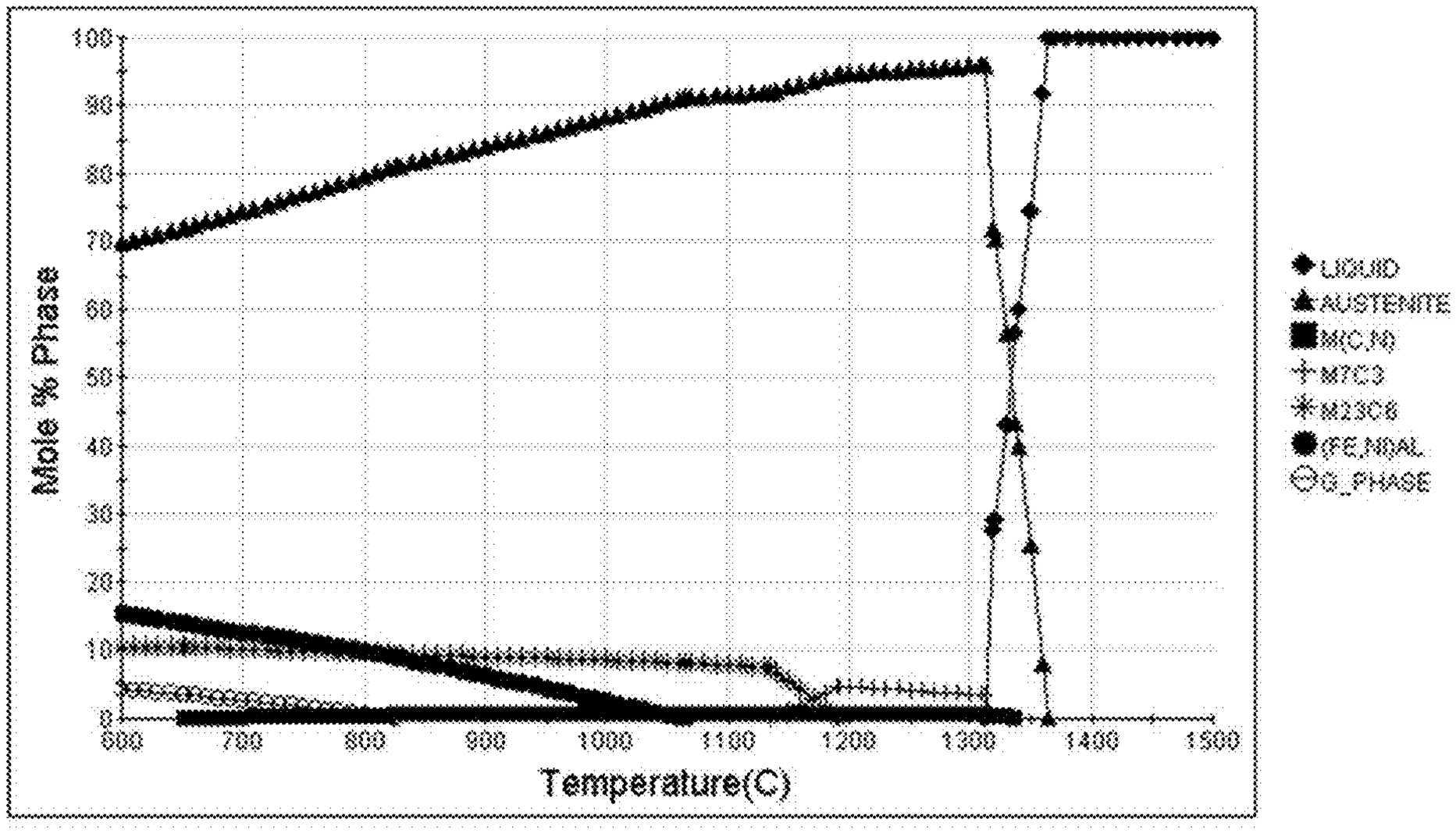
Mole % Phase
Temperature(C)
100
90
80
70
60
50
40
30
20
10
0
600
700
800
900
1000
1100
1200
1300
1400
1500
LIQUID
AUSTENITE
M(C,N)
M7C3
M23C6
(FE,NI)AL
G_PHASE

FIG. 31

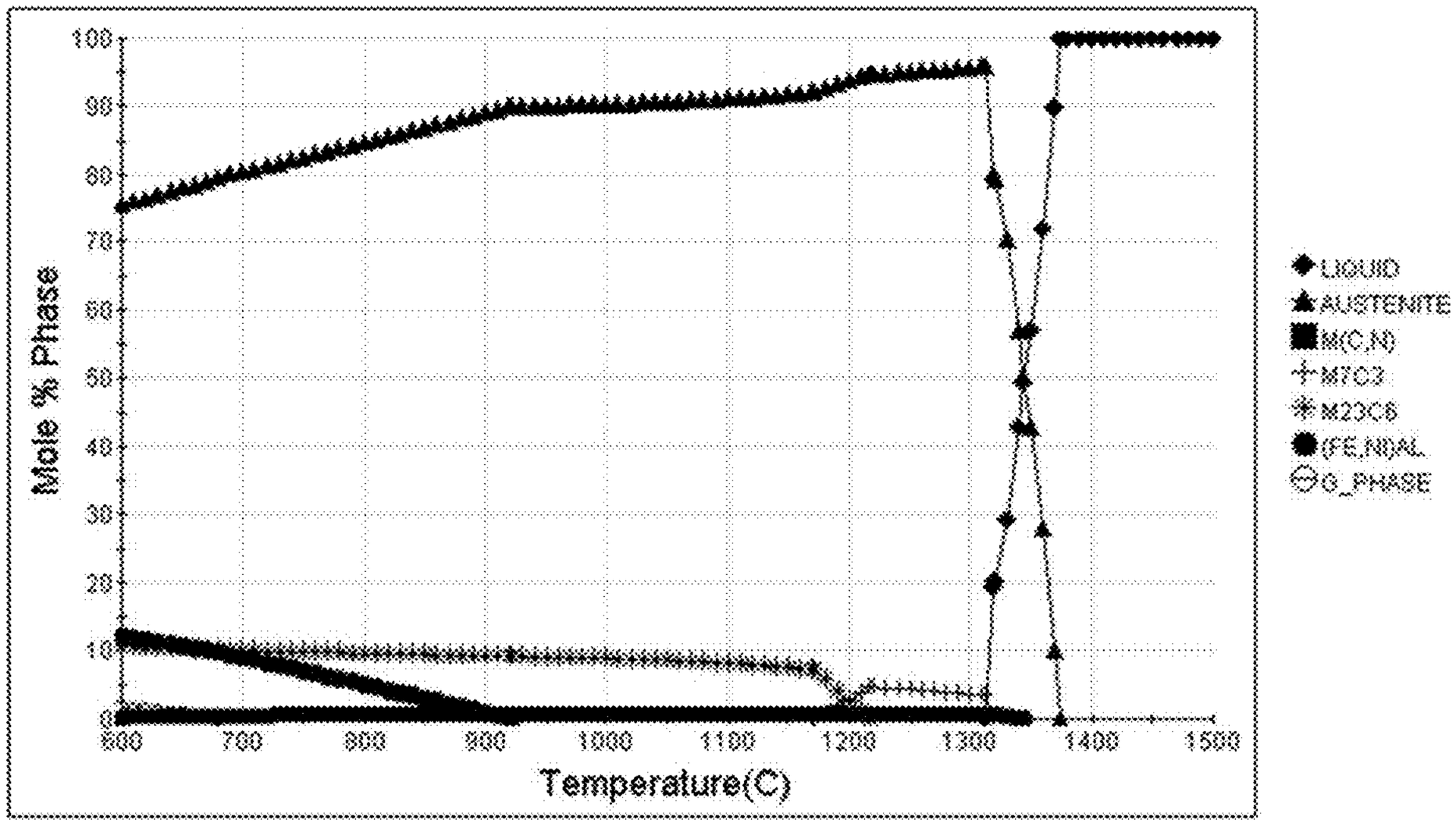
Mole % Phase
100
90
80
70
60
50
40
30
20
10
0
500
700
900
1100
1000
1100
1200
1300
1400
1500
Temperature(C)
LIQUID
AUSTENITE
M(C,N)
M7C3
M23C6
(FE,NI)AL
G_PHASE

FIG. 32

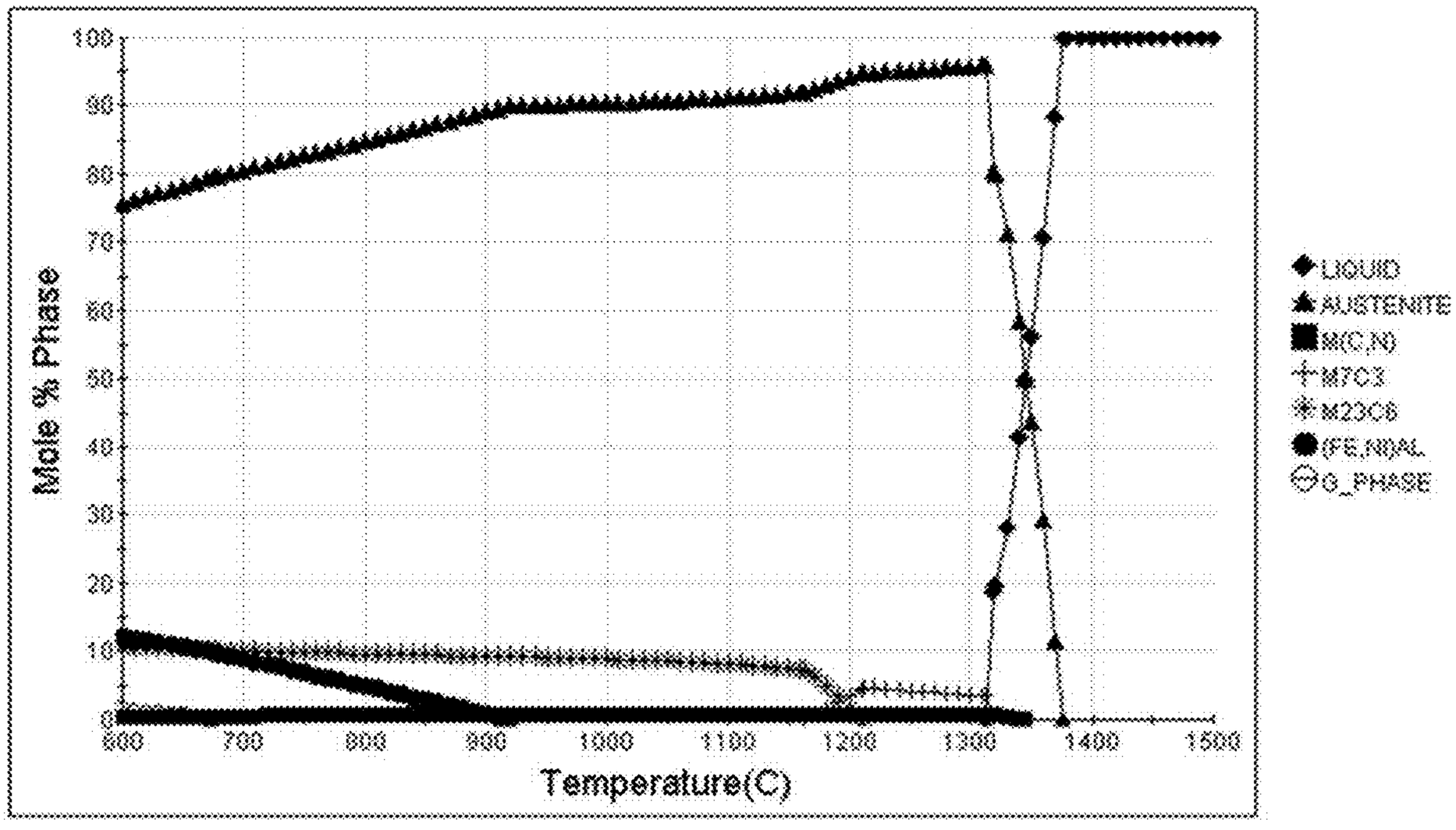
Mole % Phase
Temperature(C)
100
90
80
70
60
50
40
30
20
10
0
600
700
800
900
1000
1100
1200
1300
1400
1500
LIQUID
AUSTENITE
M(C,N)
M7C3
M23C6
(FE,NI)AL
G_PHASE

FIG. 33

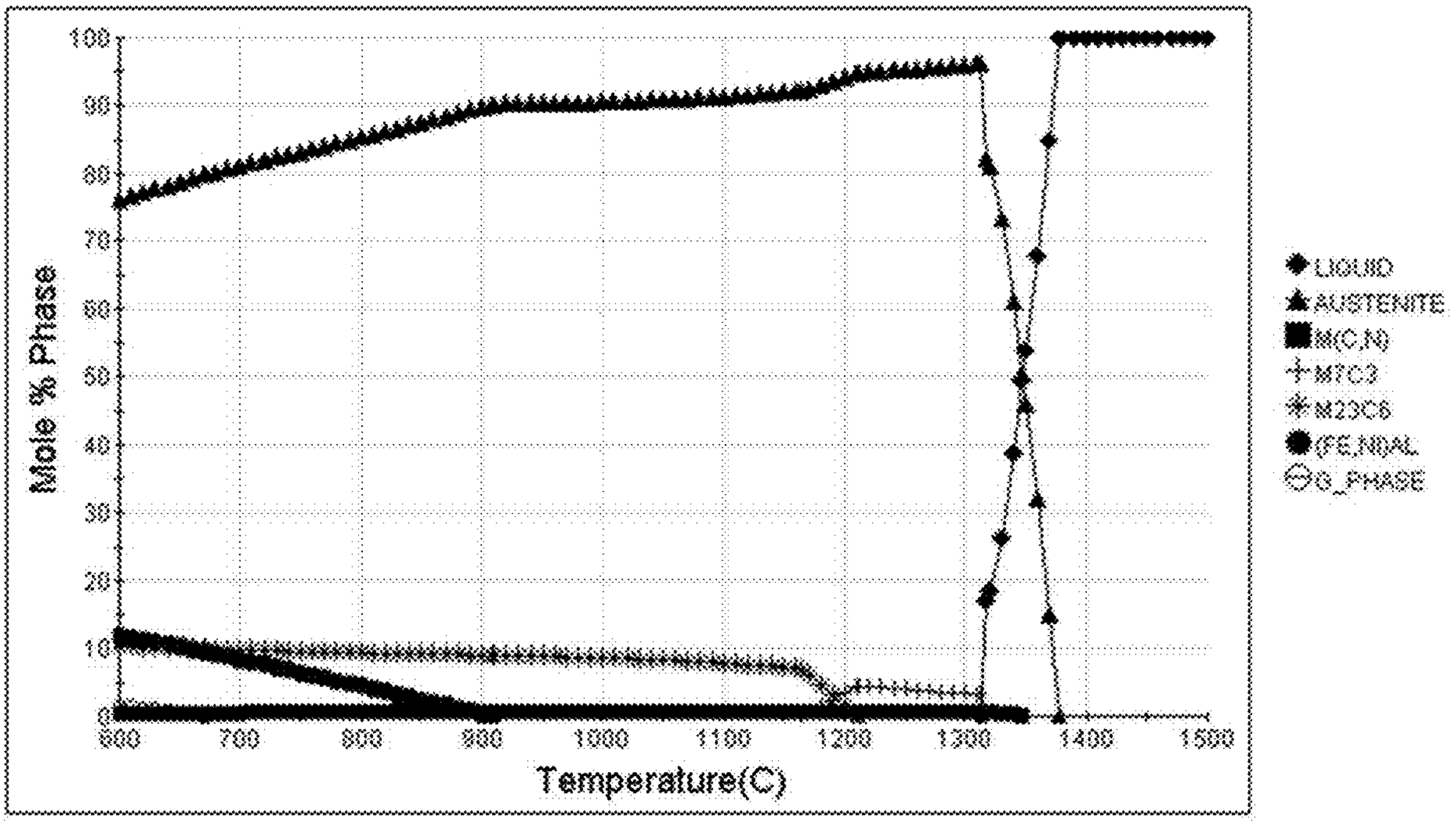
Mole % Phase
100
90
80
70
60
50
40
30
20
10
0
600
700
800
900
1000
1100
1200
1300
1400
1500
Temperature(C)
LIQUID
AUSTENITE
M(C,N)
M7C3
M23C6
(FE,NB)AL
G_PHASE

FIG. 34

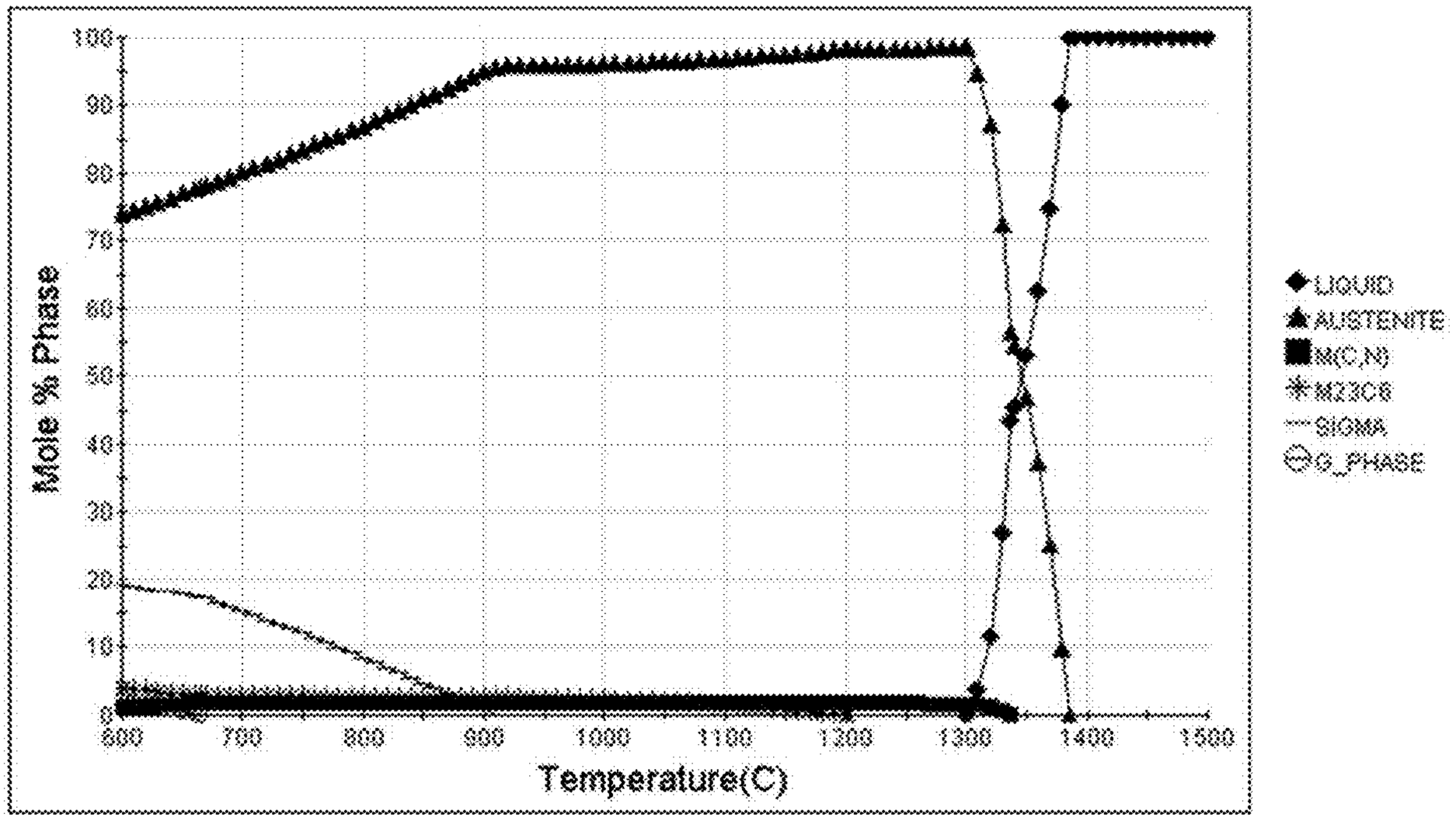
Mole % Phase
100
90
80
70
60
50
40
30
20
10
0
600
700
800
900
1000
1100
1200
1300
1400
1500
Temperature(C)
LIQUID
AUSTENITE
M(C,N)
M23C6
SIGMA
G_PHASE

FIG. 35

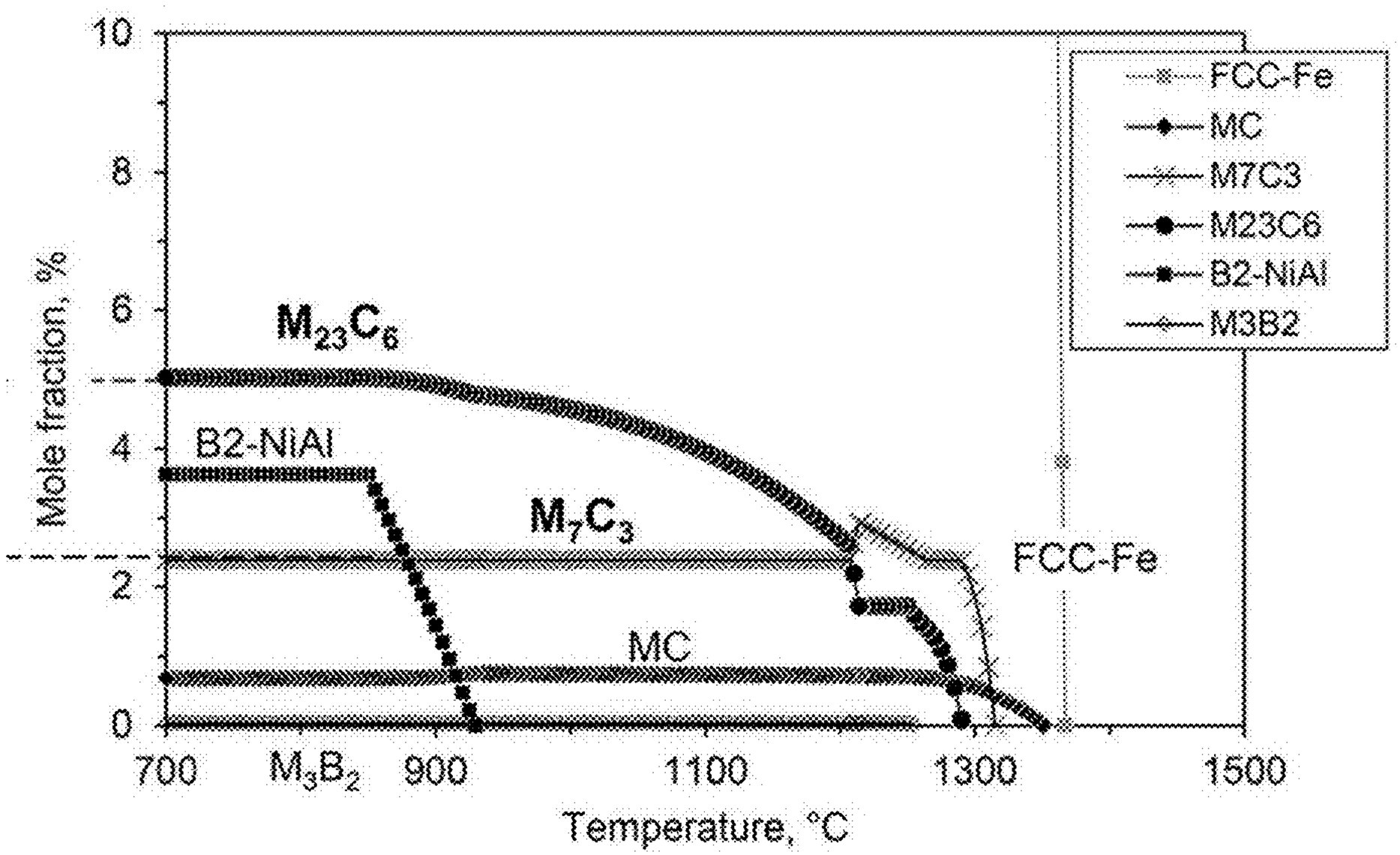
10
8
6
4
2
0
Mole fraction, %
$M_{23}C_6$
B2-NiAl
M_7C_3
MC
FCC-Fe
700
M_3B_2
900
1100
1300
1500
Temperature, °C
FCC-Fe
MC
M7C3
M23C6
B2-NiAl
M3B2

FIG. 36

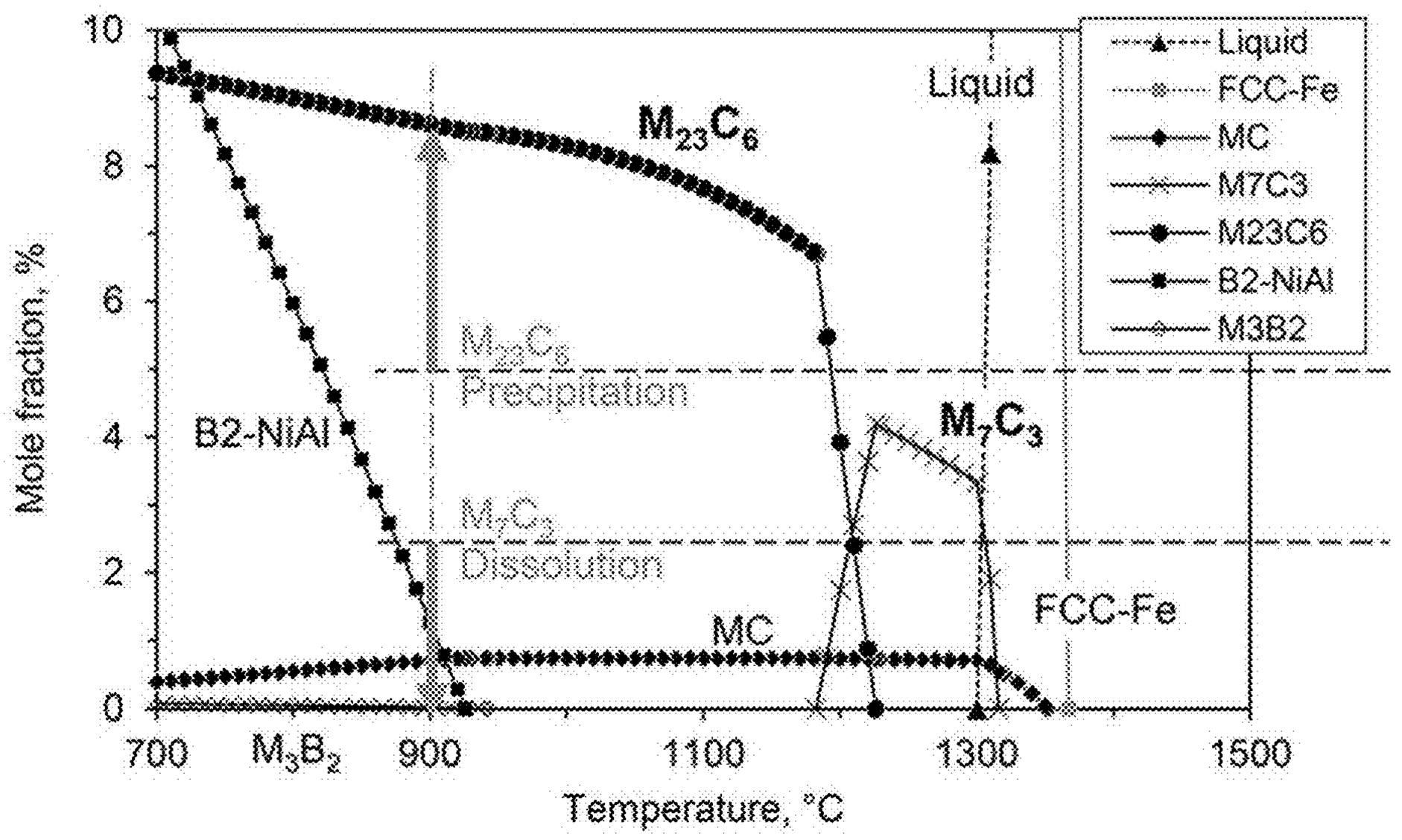
Liquid
FCC-Fe
MC
M7C3
M23C6
B2-NiAl
M3B2
Liquid
$M_{23}C_6$
$M_{23}C_6$ Precipitation
M_7C_3
B2-NiAl
M_7C_3 Dissolution
FCC-Fe
MC
M_3B_2
Mole fraction, %
Temperature, °C
0
2
4
6
8
10
700
900
1100
1300
1500

FIG. 37

CAST IRON-BASE, HIGH-STRENGTH, OXIDATION-RESISTANT ALLOY

CROSS-REFERENCE TO RELATED APPLICATIONS

[0001] This application claims priority to U.S. 63/399,233 filed Aug. 19, 2022, entitled "CAST IRON-BASE, HIGH-STRENGTH, OXIDATION-RESISTANT ALLOY", the entire disclosure of which incorporated herein by reference.

STATEMENT REGARDING FEDERALLY SPONSORED RESEARCH AND DEVELOPMENT

[0002] This invention was made with government support under Contract No. DE-AC05-00OR22725 awarded by the U.S. Department of Energy. The government has certain rights in this invention.

FIELD OF THE INVENTION

[0003] The present invention relates to oxidation-resistant alloys, and more particularly to cast iron-based alloys.

BACKGROUND OF THE INVENTION

[0004] Common austenitic stainless steels contain a maximum by weight percent of 0.15% carbon, a minimum of 16% chromium and sufficient nickel and/or manganese to retain a face centered-cubic (FCC) austenitic crystal structure at cryogenic temperatures through the melting point of the alloy. Austenitic stainless steels are non-magnetic non-heat-treatable steels that are usually annealed and cold worked. Common austenitic stainless steels are widely used in power generating applications; however, they are becoming increasingly less desirable as the industry moves toward higher thermal efficiencies. Higher operating temperatures in power generation result in reduced emissions and increased efficiencies. Conventional austenitic stainless steels currently offer good creep strength and environmental resistance up to 600-700° C. However, in order to meet emission and efficiency goals of the next generation of power plants structural alloys will be needed to increase operating temperatures by 50-100° C.

[0005] Austenitic stainless steels for high temperature use rely on chromium-oxide (chromia, Cr_2O_3) scales for oxidation protection. These scales grow relatively quickly. However, compromised oxidation resistance of chromia in the presence of aggressive species such as water vapor, carbon, sulfur, and the like typically encountered in energy production and process environments necessitates a reduction in operating temperature to achieve component durability targets. This temperature reduction reduces process efficiency and increases environmental emissions.

[0006] High nickel austenitic stainless steels and nickel-based superalloys can meet the required property targets, but their costs for construction of power plants are prohibitive due to the high cost of nickel. Creep failure of common austenitic stainless steels such as types 316, 321, and 347 limits their use in these higher temperature applications.

[0007] A new class of austenitic stainless steels has been recently developed to be more oxidation resistant at higher temperature—these are the alumina-forming austenitic (AFA) stainless steels. These alloys are described in Yamamoto et al. U.S. Pat. No. 7,754,305, Brady et al U.S. Pat. No. 7,744,813, and Brady et al U.S. Pat. No. 7,754,144, Muralidharan U.S. Pat. No. 8,431,072, and Yamamoto U.S. Pat. No. 8,815,146, and U.S. Pub. No. 2022/0251690, the disclosures of which are hereby incorporated fully by reference.

[0008] Alumina-forming austenitic (AFA) stainless steels are a new class of high-temperature (600-1150° C.) structural alloy steels with a wide range of energy production, chemical/petrochemical, and process industry applications. These steels combine the relatively low cost, excellent formability, weldability, and good high-temperature creep strength (resistance to sagging over time) of state-of-the-art advanced austenitic stainless steels with fundamentally superior high-temperature oxidation (corrosion) resistance due to their ability to form protective aluminum oxide (alumina, Al_2O_3) surface layers.

[0009] Alumina grows at a rate 1 to 2 orders of magnitude lower than chromia and is also significantly more thermodynamically stable in oxygen, which results in its fundamentally superior high-temperature oxidation resistance. A further, key advantage of alumina over chromia is its greater stability in the presence of water vapor. Water vapor is encountered in most high-temperature industrial environments, ranging, for example, from gas turbines, combustion, and fossil-fired steam plants to solid oxide fuel cells. With both oxygen and water vapor present, volatile chromium oxy-hydroxide species can form and significantly reduce oxidation lifetime, necessitating significantly lower operating temperatures. This results in reduced process efficiency and increased emissions.

[0010] Many applications require complicated component shapes best achieved by casting (engine and turbine components). Casting can also result in lower cost tube production methods for chemical/petrochemical and power generation applications. To date cast AFA alloy development has focused on higher Ni (greater than or equal to 35 wt. % Ni alloys).

[0011] Cast alloys for use in the temperature range of about 900-1100° C. are needed for applications such as furnace tubes, furnace rolls, and petrochemical applications. One example of this class of materials is Cast HP—Nb type alloy of the composition. These alloys contain about 35 wt. % Ni and about 25 wt. % Cr, 1 wt. % Nb, 1 wt. % Si, with up to ~0.45 wt. % carbon. These obtain their creep resistance through the formation of carbides. They also obtain their oxidation resistance through the formation of chromia scales. Another common alloy consists of 45 wt. % Ni and about 35 wt. % Cr with about 1 wt. % Nb, 1 wt. % Si, and 0.45 wt. % C and is widely used in the petrochemical industry.

[0012] The AFA alloy composition range represents a series of trade-offs between the creep strength and the ability to form protective alumina. AFA alloys exhibit a transition to nonprotective oxidation and internal oxidation and nitridation of Al, instead of a continuous protective surface layer of alumina, with increasing temperatures. The transition temperature can vary from 700-750° C. to greater than 1100° C. depending on the alloy composition, with higher levels of Al, Cr, Ni, and Nb favoring higher temperature oxidation resistance, but with higher cost due to the expense of Ni and Nb, and frequently lower creep resistance.

[0013] Automotive exhaust components are anticipated to experience higher temperatures to reach engine efficiency targets. The ferrous cast alloys currently used for turbocharger housings and exhaust manifolds are at their upper-temperature limit for creep and/or oxidation resistance.

Therefore, new, cost-effective alloys will be required to meet the increasing operating temperature requirements in higher efficiency engines, including reciprocating engines fueled by hydrogen.

SUMMARY OF THE INVENTION

[0014] An AFA alloy composition can comprise, consist essentially of, or consist of:

[0015] 0.4 to 0.59 Nb+Ta;

[0016] 0.4 to 0.6 C

[0017] 16 o 18 Cr

[0018] 18-23 Ni

[0019] 3.5-5.5 Al

[0020] 0.005-0.15 B

[0021] up to 1.5 Mo

[0022] up to 2 Co;

[0023] up to 1 W;

[0024] up to 3 Cu;

[0025] up to 4 Mn;

[0026] up to 2 Si;

[0027] up to 0.5 wt. % total of at least one element selected from the group consisting of Ti and V;

[0028] up to 0.06 N;

[0029] up to 1 wt. % total of at least one element selected from the group consisting of Y, La, Ce, Hf, and Zr;

[0030] balance Fe, wherein the weight percent Fe is greater than the weight percent Ni, and wherein said alloy forms an external continuous scale comprising alumina to at least 900° C. in air with 10% H_2O, and a stable essentially single phase FCC austenitic matrix microstructure, said austenitic matrix being essentially delta-ferrite free and essentially BCC-phase-free, with creep rupture life in excess of 500 h at 900° C. and 50 MPa.

[0031] The alloy can have a creep rupture life greater than 1000 h at 900° C. and 50 MPa. The alloy can have a yield strength at 900° C. that is greater than 18.75 ksi. The alloy can have a yield strength at 900° C. that is greater than 21 ksi.

[0032] The alloy can have an ultimate tensile strength that is greater than 22.75 ksi. The alloy can have an ultimate tensile strength is greater than 26 ksi. The alloy can have a mass gain after exposure to air with 10 vol % H_2O at 950° C. in 1 h cycles for 1000 h is less than 1 mg/cm^2. The alloy can have a mass gain after exposure to air with 10 vol % H_2O at 1000° C. in 1 h cycles for 500 h is less than 1 mg/cm^2.

[0033] The alloy can have an atomic ratio R that is from 3.77 to 4.77. The can have an atomic ratio R that is from 4.42 to 4.77. The alloy can have a calculated equilibrium mole % at 900° C. of MC carbides is from 0.31 to 0.67.

[0034] The alloy can have a calculated equilibrium mole % at 900° C. of $M_{23}C_6$ carbides that is from 8.56 to 9.86. The alloy can have a calculated equilibrium mole % at 900° C. of MC and $M_{23}C_6$ carbides is from 9.19 to 10.24. The alloy can have a calculated change in mole % of total carbides is from 5.46 to 6.33. The alloy can have a calculated change in mole % of MC and $M_{23}C_6$ is from 6.86 to 8.61.

BRIEF DESCRIPTION OF THE DRAWINGS

[0035] There are shown in the drawings embodiments that are presently preferred it being understood that the invention is not limited to the arrangements and instrumentalities shown, wherein:

[0036] FIG. **1** is a plot of oxidation data as specific mass change (mg/cm^2) vs. exposure time at 900° C. in air with 10% H_2O, with exposures conducted in 1-h cycles.

[0037] FIG. **2** is a plot of oxidation data as specific mass change (mg/cm^2, isolating and enlarging 0 to 1) vs. exposure time at 900° C. in air with 10% H_2O, with exposures conducted in 1-h cycles.

[0038] FIG. **3** is a plot of oxidation data as specific mass change (mg/cm^2) vs. exposure time at 950° C. in air with 10% H_2O, with exposures conducted in 1-h cycles.

[0039] FIG. **4** is a plot of oxidation data as specific mass change (mg/cm^2) vs. exposure time at 1000° C. in air with 10% H_2O, with exposures conducted in 1-h cycles.

[0040] FIG. **5** is a scanning electron microscopy (SEM) cross-section image of the oxide scale formed on AFA5 after 1000, 1-h cycles at 950° C. in air with 10% H_2O showing continuous scale formation.

[0041] FIG. **6** is a scanning transmission electron microscopy (STEM) cross-section image of the oxide scale formed on AFA 5 after 1000, 1-h cycles at 950° C. in air with 10% H_2O showing continuous scale formation.

[0042] FIG. **7** is an Al elemental map of the oxide scale formed on AFA 5 after 1000, 1-h cycles at 950° C. in air with 10% H_2O.

[0043] FIG. **8** is an O elemental map of the oxide scale formed on AFA 5 after 1000, 1-h cycles at 950° C. in air with 10% H_2O.

[0044] FIG. **9** is a bar chart showing the yield strength and the ultimate tensile strength at 900° C. of AFA1, AFA2, AFA3 and AFA5 and reference alloy 1.4826.

[0045] FIG. **10** shows the creep rupture life (h) at 900° C. and 50 MPa for lab cast alumina-forming AFA 2 and AFA 5 relative to commercial chromia-forming 1.4826 (Fe-11Ni-22Cr base), HK (Fe-20Ni-25Cr base), and HP (Fe-35Ni-25Cr base) commercial alloys. Creep rupture life data for the chromia-formers was based on estimates from literature data.

[0046] FIG. **11** shows the mass change (mg/cm^2) after 1000 h of exposure during cyclic oxidation testing at 950° C. in air with 10% water vapor in 1 h cycles as a function of Ni content in the alloy.

[0047] FIG. **12** shows the mass change (mg/cm^2) after 500 h of exposure during cyclic oxidation testing at 1000° C. in air with 10% water vapor in 1 h cycles as a function of Ni content in the alloy.

[0048] FIG. **13** shows the mass change (mg/cm^2) after 1000 h of exposure during cyclic oxidation testing at 950° C. in air with 10% water vapor in 1 h cycles as a function of Nb content in the alloy.

[0049] FIG. **14** shows the mass change (mg/cm^2) after 100 h of exposure during cyclic oxidation testing at 1000° C. in air with 10% water vapor in 1 h cycles as a function of Nb content in the alloy.

[0050] FIG. **15** shows the mass change (mg/cm^2) after 500 h of exposure during cyclic oxidation testing at 950° C. in air with 10% water vapor in 1 h cycles as a function of Al and Si contents in the alloy.

[0051] FIG. **16** shows the mass change (mg/cm^2) after 500 h of exposure during cyclic oxidation testing at 1000° C. in air with 10% water vapor in 1 h cycles as a function of Y content in the alloy.

[0052] FIG. **17** is a bar chart showing a comparison of creep-rupture lives of cast AFA 5 alloys (lab-scale heats) and reference HK30Nb alloy tested at 900° C. and 50 MPa.

[0053] FIG. **18** is a plot showing the creep rupture lives at 900° C. and 500 MPa as a function of the atomic ratio R.

[0054] FIG. **19** is a plot showing creep-rupture lives (h) tested at 900° C. and 50 Mpa, and a bar chart showing mass gains (mg/cm^2), after total 1000 h exposure at 950° C. in air with 10% water vapor environment in AFA 5 base alloys, plotted as a function of the Nb composition.

[0055] FIG. **20** is a calculated equilibrium phase diagram in mol % as a function of temperature (° C.) for the alloy AFA1.

[0056] FIG. **21** is a calculated equilibrium phase diagram in mol % as a function of temperature (° C.) for the alloy AFA2.

[0057] FIG. **22** is a calculated equilibrium phase diagram in mol % as a function of temperature (° C.) for the alloy AFA3.

[0058] FIG. **23** is a calculated equilibrium phase diagram in mol % as a function of temperature (° C.) for the alloy AFA5.

[0059] FIG. **24** is a calculated equilibrium phase diagram in mol % as a function of temperature (° C.) for the alloy AFA5Nb1. in mol % as a function of temperature (° C.)

[0060] FIG. **25** is a calculated equilibrium phase diagram in mol % as a function of temperature (° C.) for the alloy AFA5Nb2.

[0061] FIG. **26** is a calculated equilibrium phase diagram in mol % as a function of temperature (° C.) for the alloy AFA5Nb3.

[0062] FIG. **27** is a calculated equilibrium phase diagram in mol % as a function of temperature (° C.) for the alloy AFA5Ni0.

[0063] FIG. **28** is a calculated equilibrium phase diagram in mol % as a function of temperature (° C.) for the alloy AFA5Ni1.

[0064] FIG. **29** is a calculated equilibrium phase diagram in mol % as a function of temperature (° C.) for the alloy AFA5Ni2.

[0065] FIG. **30** is a calculated equilibrium phase diagram in mol % as a function of temperature (° C.) for the alloy AFA5Si1.

[0066] FIG. **31** is a calculated equilibrium phase diagram in mol % as a function of temperature (° C.) for the alloy AFA5Si2.

[0067] FIG. **32** is a calculated equilibrium phase diagram in mol % as a function of temperature (° C.) for the alloy AFA5Y1.

[0068] FIG. **33** is a calculated equilibrium phase diagram in mol % as a function of temperature (° C.) for the alloy AFA5Y2.

[0069] FIG. **34** is a calculated equilibrium phase diagram in mol % as a function of temperature (° C.) for the alloy AFA5Y3.

[0070] FIG. **35** is a calculated equilibrium phase diagram in mol % as a function of temperature (° C.) for the alloy HK30Nb.

[0071] FIG. **36** is a plot of mole fraction % vs. temperature (° C.) obtained for the cast AFA 5 alloy showing the phases predicted to appear during solidification.

[0072] FIG. **37** is a plot of thermodynamic calculation results of the cast AFA 5 alloy series showing the amounts of equilibrated and as-solidified mole fraction % of $M_{23}C_6$.

DETAILED DESCRIPTION OF THE INVENTION

[0073] A cast AFA alloy composition according to the invention can comprise, in weight percent based on the total weight of the alloy:

[0074] 0.4 to 0.59 Nb+Ta;

[0075] 0.4 to 0.6 C;

[0076] 16 to 18 Cr;

[0077] 18-23 Ni;

[0078] 3.5-5.5 Al;

[0079] 0.005 to 0.15 B;

[0080] up to 1.5 Mo;

[0081] up to 2 Co;

[0082] up to 1 W;

[0083] up to 3 Cu;

[0084] up to 4 Mn;

[0085] up to 2 Si;

[0086] up to 0.5 wt. % total of at least one element selected from the group consisting of Ti and V;

[0087] up to 0.06 N;

[0088] up to 1 wt. % total of at least one element selected from the group

[0089] consisting of Y, La, Ce, Hf, and Zr;

balance Fe, wherein the weight percent Fe is greater than the weight percent Ni, and wherein the alloy forms an external continuous scale comprising alumina to at least 900° C. in air with 10% H_2O, and a stable essentially single-phase FCC austenitic matrix microstructure, the austenitic matrix being essentially delta-ferrite free and essentially BCC-phase-free, with creep rupture life in excess of 500 h at 900° C. and 50 MPa.

[0090] The Nb+Ta in weight percent can be 0.4, 0.41, 0.42, 0.43, 0.44, 0.45, 0.46, 0.47, 0.48, 0.49, 0.5, 0.51, 0.52, 0.53, 0.54, 0.55, 0.56, 0.57, 0.58, or 0.59. The Nb+Ta can be in a range of any high value and low value selected from these values.

[0091] The C in weight percent can be 0.4, 0.41, 0.42, 0.43, 0.44, 0.45, 0.46, 0.47, 0.48, 0.49, 0.5, 0.51, 0.52, 0.53, 0.54, 0.55, 0.56, 0.57, 0.58, 0.59, or 0.6. The C can be in a range of any high value and low value selected from these values.

[0092] The Cr in weight percent can be 16, 16.1, 16.2, 16.3, 16.4, 16.5, 16.6, 16.7, 16.8, 16.9, 17, 17.1, 17.2, 17.3, 17.4, 17.5, 17.6, 17.7, 17.8, 17.9 or 18. The Cr can be in a range of any high value and low value selected from these values.

[0093] The Ni in weight percent can be 18, 18.1, 18.2, 18.3, 18.4, 18.5, 18.6, 18.7, 18.8, 18.9, 19, 19.1, 19.2, 19.3, 19.4, 19.5, 19.6, 19.7, 19.8, 19.9, 20, 20.1, 20.2, 20.3, 20.4, 20.5, 20.6, 20.7, 20.8, 20.9, 21, 21.1, 21.2, 21.3, 21.4, 21.5, 21.6, 21.7, 21.8, 21.9, 22, 22.1, 22.3, 22.4, 22.5, 22.6, 22.7, 22.8, 22.9 or 23. The Ni can be in a range of any high value and low value selected from these values.

[0094] The Al in weight percent can be 3.5, 3.6, 3.7, 3.8, 3.9, 4, 4.1, 4.2, 4.3, 4.4, 4.5, 4.6, 4.7, 4.8, 4.9, 5, 5.1, 5.2, 5.3, 5.4 or 5.5. The Al can be in a range of any high value and low value selected from these values.

[0095] The B in weight percent can be 0.005, 0.010, 0.015, 0.020, 0.025, 0.030, 0.035, 0.040, 0.045, 0.050, 0.055, 0.060, 0.065, 0.070, 0.075, 0.080, 0.085, 0.090, 0.095, 0.100, 0.105, 0.110, 0.115, 0.120, 0.125, 0.130, 0.135, 0.140, 0.145, or 1.150. The B can be in a range of any high value and low value selected from these values.

[0096] The Mo in weight percent can be 0, 0.1, 0.2, 0.3, 0.4, 0.5, 0.6, 0.7, 0.8, 0.9, 1.0, 1.1, 1.2, 1.3, 1.4, or 1.5. The Mo can be in a range of any high value and low value selected from these values.

[0097] The Co in weight percent can be 0, 0.1, 0.2, 0.3, 0.4, 0.5, 0.6, 0.7, 0.8, 0.9, 1.0, 1.1, 1.2, 1.3, 1.4, 1.5, 1.6, 1.7, 1.8, 1.9, or 2.0. The Co can be in a range of any high value and low value selected from these values.

[0098] The Win weight percent can be 0, 0.05, 0.1, 0.15, 0.2, 0.25, 0.3, 0.35, 0.4, 0.45, 0.5, 0.55, 0.6, 0.65, 0.7, 0.75, 0.8, 0.85, 0.9, 0.95, or 1.0. The W can be in a range of any high value and low value selected from these values.

[0099] The Cu in weight percent can be 0, 0.1, 0.2, 0.3, 0.4, 0.5, 0.6, 0.7, 0.8, 0.9, 1.0, 1.1, 1.2, 1.3, 1.4, 1.5, 1.6, 1.7, 1.8, 1.9, 2.0, 2.1, 2.2, 2.3, 2.4, 2.5, 2.6, 2.7, 2.8, 2.9, or 3.0. The Cu can be in a range of any high value and low value selected from these values.

[0100] The Mn in weight percent can be 0, 0.1, 0.2, 0.3, 0.4, 0.5, 0.6, 0.7, 0.8, 0.9, 1.0, 1.1, 1.2, 1.3, 1.4, 1.5, 1.6, 1.7, 1.8, 1.9, 2.0, 2.1, 2.2, 2.3, 2.4, 2.5, 2.6, 2.7, 2.8, 2.9, 3.0, 3.1, 3.2, 3.3, 3.4, 3.5, 3.6, 3.7, 3.8, 3.9, or 4.0. The Mn can be in a range of any high value and low value selected from these values.

[0101] The Si in weight percent can be 0, 0.1, 0.2, 0.3, 0.4, 0.5, 0.6, 0.7, 0.8, 0.9, 1.0, 1.1, 1.2, 1.3, 1.4, 1.5, 1.6, 1.7, 1.8, 1.9, or 2.0. The Si can be in a range of any high value and low value selected from these values.

[0102] The combined Y, La, Ce, Hf and/or Zr can be 0, 0.05, 0.1, 0.15, 0.2, 0.25, 0.3, 0.35, 0.4, 0.45, 0.5, 0.55, 0.6, 0.65, 0.7, 0.75, 0.8, 0.85, 0.9, 0.95, or 1.0. The combined Y, La, Ce, Hf and/or Zr can be in a range of any high value and low value selected from these values.

[0103] N in weight % can be found within the range of 0, 0.002, 0.004, 0.006, 0.008, 0.01, 0.012, 0.014, 0.016, 0.018, 0.02, 0.022, 0.024, 0.026, 0.028, 0.03, 0.032, 0.034, 0.036, 0.038, 0.04, 0.042, 0.044, 0.046, 0.048, 0.05, 0.052, 0.054, 0.056, 0.058 or 0.06 N %. N can have a weight % within a range of any high value and low value selected from these values.

[0104] Ti and V, independently or collectively, can be up to 0.5 wt. %. Ti and V can be 0, 0.01, 0.02, 0.03, 0.04, 0.05, 0.06, 0.07, 0.08, 0.09, 0.1, 0.11, 0.12, 0.13, 0.14, 0.15, 0.16, 0.17, 0.18, 0.19, 0.2, 0.22, 0.24, 0.26, 0.28, 0.3, 0.32, 0.34, 0.36, 0.38, 0.4, 0.42, 0.44, 0.46, 0.48, or 0.5 wt. %. The Ti and V can be within a range of any high value and low value selected from these values.

[0105] The mass gain after exposure to air with 10 vol % H_2O at 950° C. in 1 h cycles for 1000 h can be less than 1 mg/cm^2. The mass gain after exposure to air with 10 vol % H_2O at 950° C. in 1 h cycles for 1000 h can be 0, 0.05, 0.10, 0.15, 0.20, 0.25, 0.30, 0.35, 0.40, 0.45, 0.5, 0.55, 0.6, 0.65, 0.7, 0.75, 0.8, 0.85, 0.9, 0.95 or 1. The mass gain after exposure to air with 10 vol % H_2O at 950° C. in 1 h cycles for 1000 h can be within a range of any high value and low value selected from these values.

[0106] The mass gain after exposure to air with 10 vol % H_2O at 1000° C. in 1 h cycles for 500 h is less than 1 mg/cm^2. The mass gain after exposure to air with 10 vol % H_2O at 1000° C. in 1 h cycles for 500 h is less than 1 mg/cm^2 can be 0, 0.05, 0.10, 0.15, 0.20, 0.25, 0.30, 0.35, 0.40, 0.45, 0.5, 0.55, 0.6, 0.65, 0.7, 0.75, 0.8, 0.85, 0.9, 0.95 or 1. The mass gain after exposure to air with 10 vol % H_2O at 1000° C. in 1 h cycles for 500 h can be within a range of any high value and low value selected from these values.

[0107] The alloy can have an atomic ratio R from 3.77 to 4.77. The alloy can have an atomic ratio R of 3.77, 3.8, 3.85, 3.9, 3.95, 4, 4.05, 4.1, 4.15, 4.2, 4.25, 4.3, 4.35, 4.4, 4.45, 4.5, 4.55, 4.6, 4.65, 4.7, 4.75 or 4.77. The atomic ratio R can be within a range of any high value and low value selected from these values.

[0108] The calculated equilibrium mole % at 900° C. of MC carbides can be from 0.31 to 0.67. The calculated equilibrium mole % at 900° C. of MC carbides can be 0.31, 0.35, 0.4, 0.45, 0.5, 0.55, 0.6, 0.65, or 0.67. The calculated equilibrium mole % at 900° C. of MC carbides can be within a range of any high value and low value selected from these values.

[0109] The calculated equilibrium mole % at 900° C. of $M_{23}C_6$ carbides is from 8.56 to 9.86. The calculated equilibrium mole % at 900° C. of $M_{23}C_6$ carbides can be 8.56, 8.6, 8.65, 8.7, 8.75, 8.8, 8.85, 8.9, 8.95, 9, 9.05, 9.1, 9.15, 9.2, 9.25, 9.3, 9.35, 9.4, 9.45, 9.5, 9.55, 9.6, 9.65, 9.7, 9.75, 9.8, or 9.86. The calculated equilibrium mole % at 900° C. of $M_{23}C_6$ carbides can be within a range of any high value and low value selected from these values.

[0110] The calculated equilibrium mole % at 900° C. of MC and $M_{23}C_6$ carbides can be from 9.19 to 10.24. The calculated equilibrium mole % at 900° C. of MC and $M_{23}C_6$ carbides can be 9.19, 9.25, 9.3, 9.35, 9.4, 9.45, 9.5, 9.55, 9.6, 9.65, 9.7, 9.75, 9.8, 9.85, 9.9, 9.95, 10, 10.05, 10.1, 110.15, 10.2, or 10.24. The calculated equilibrium mole % at 900° C. of MC and $M_{23}C_6$ carbides can be within a range of any high value and low value selected from these values.

[0111] The calculated change in mole % of total carbides can be from 5.46 to 6.33. The calculated change in mole % of total carbides can be 5.46, 5.5, 5.55, 5.6, 5.65, 5.7, 5.75, 5.8, 5.85, 5.9, 5.95, 6, 6.05, 6.1, 6.15, 6.2, 6.25, 6.3, or 6.33. The calculated change in mole % of total carbides can be within a range of any high value and low value selected from these values.

[0112] The calculated change in mole % of MC and $M_{23}C_6$ can be from 6.86 to 8.61. The calculated change in mole % of MC and $M_{23}C_6$ can be 6.86, 6.9, 7, 7.1, 7.2, 7.3, 7.4, 7.5, 7.6, 7.7, 7.8, 7.9, 8, 8.1, 8.2, 8.3, 8.4, 8.5, or 8.61. The calculated change in mole % of MC and $M_{23}C_6$ can be within a range of any high value and low value selected from these values.

[0113] Alumina-forming austenitic (AFA) stainless steels are a class of structural steel alloys which comprise aluminum (Al) at a weight percentage sufficient to form protective aluminum oxide (alumina, Al_2O_3) surface layers. The external continuous scale comprising alumina does not form at an Al level below about 2 weight percent. At an Al level higher than about 3.5 to 5.5 weight percent, the exact transition dependent on level of austenite stabilizing additions such as Ni (e.g. higher Ni can tolerate more Al), a significant bcc phase is formed in the alloy, which compromises the high temperature properties of the alloy such as creep strength. The external alumina scale is continuous at the alloy/scale interface and though Al_2O_3 rich the scale can contain some

Mn, Cr, Fe and/or other metal additives such that the growth kinetics of the Al rich oxide scale is within the range of that for known alumina scale.

[0114] Nitrogen is found in some conventional Cr_2O_3-forming grades of austenitic alloys up to about 0.5 wt. % to enhance the strength of the alloy. The nitrogen levels in AFA alloys must be kept as low as possible to avoid detrimental reaction with the Al and achieve alloys which display oxidation resistance and high creep strength at high temperatures. Although processing will generally result in some uptake of N in the alloy, it is necessary to keep the level of N at less than about 0.06 wt % for the inventive alloys. When N is present, the Al forms internal nitrides, which can compromise the formation of the alumina scale needed for the desired oxidation resistance as well as a good creep resistance.

[0115] The addition of Ti and/or V is common to virtually all high-temperature austenitic stainless steels and related alloys to obtain high temperature creep strength, via precipitation of carbide and related phases. To permit the formation of the alloys of the invention and the alumina scale, the composition typically has to include little or no titanium or vanadium, with a combined level of less than about 0.5 weight percent. The addition of Ti and V shifts the oxidation behavior (possibly by increasing oxygen permeability) in the alloy such that Al is internally oxidized, requiring much higher levels of Al to form an external Al_2O_3 scale in the presence of Ti and V. At such high levels, the high temperature strength properties of the resulting alloy are compromised by stabilization of the weak bcc Fe phase.

[0116] Additions of Nb or Ta are necessary for alumina-scale formation. Too much Nb or Ta will negatively affect creep properties by promoting δ-Fe and brittle second phases.

[0117] Additionally, up to 2 weight percent Co, up to 3 weight percent Cu, and up to 1.5 weight percent Mo and up to 1 wt. percent W can be present in the alloy as desired to enhance specific properties of the alloy.

[0118] Rare earth and reactive elements, such as Y, La, Ce, Hf, Zr, and the like, at a combined level of up to 1 weight percent can be included in the alloy composition as desired to enhance specific properties of the alloy. Other elements can be present as unavoidable impurities at a combined level of less than 1 weight percent.

[0119] Tolerance to nitrogen can be achieved by addition of more nitrogen active alloy additions than Al. Based on thermodynamic assessment, Hf, Ti, and Zr can be used to selectively getter N away from Al. The addition of Hf and Zr generally also offers further benefits for oxidation resistance via the well known reactive element effect, at levels up to 1 wt. %. Higher levels can result in internal oxidation and degraded oxidation resistance. Studies of AFA alloys have indicated degradation in oxidation resistance of AFA alloys with Ti and, especially, V additions or impurities, and has indicated limiting these additions to no more than 0.3 wt. % total. Assuming stoichiometric TiN formation, with 0.25 wt. % Ti, up to around 0.06 wt. % N is possible, which is sufficient to manage and tolerate the N impurities encountered in air casting. A complication is that Ti will also react with C (as will Nb). Therefore, some combination of Hf or Zr and Ti is desirable to manage and tolerate N effectively.

[0120] This invention provides a class of alumina-forming austenitic stainless steels that use one or more carbides for high temperature tensile and creep strengths. High temperature strength is obtained through the precipitation of fine carbides throughout the matrix. Creep strength is achieved through the combined precipitation of fine carbides homogeneously in the matrix that act as obstacles to motion of dislocations along with coarse carbides on grain boundaries which prevent grain boundary sliding.

[0121] Carbides can be one or more of the following-MC-type, M_7C_3 type, $M_{23}C_6$ type or others. A certain amount of coarse non-equilibrium carbides could form during solidification and additional carbides can be precipitated during high temperature exposure in service or during creep testing. Precipitation of sufficient amount of fine carbides in the matrix during high temperature exposure is required to achieve good high temperature creep resistance. These carbides must also be stable for long periods of time at high temperatures to achieve optimum creep resistance.

[0122] Within the allowable ranges of elements, particularly those of Al, Cr, Ni, Fe, Mn, Mo, Si, Nb, Ta, Ti and, when present Co, W, and Cu, the levels of the elements are adjusted relative to their respective concentrations to achieve a stable fcc austenite phase matrix. The appropriate relative levels of these elements for a composition is readily determined or checked by comparison with commercially available databases or by computational thermodynamic models with the aid of programs such as Thermo-Calc® (Thermo-Calc Software, Solna, Sweden) or JMatPro® (Sente Software, Surrey Research Park, United Kingdom). In the casting of AFA steels, the partitioning of elements during solidification determines composition control. Non-equilibrium phases formed during solidification will modify the type and amount of strengthening phases.

[0123] Elements such as Cr, Nb, Ta, Ti, V, Zr, Hf and C alone and in combinations can form carbides and elements such as W, and Mo can partition to the carbides.

[0124] Thermodynamic models can also be used to predict the type and weight % (or mole %) carbides formed during solidification and type and wt. % carbides present in equilibrium at high temperatures when the carbon levels present in the alloy are included in the calculations along with the levels of other elements. The difference between carbides present in these two conditions can be used for the calculation of carbides that precipitate during high temperature exposures. Adequate precipitation of fine carbides during high temperature exposure is required for creep strength.

[0125] In one aspect, the technology described herein provides a new cast AFA alloy compositions that yields alloys with superior combination of high temperature creep strength and oxidation resistance. The subject AFA alloys described herein exhibit both alumina formation resulting in good oxidation resistance and outstanding creep resistance to the 900-1000° C. range, but with Ni levels less than 25 wt. % and Nb levels less than 0.6 wt. %, which reduces its cost compared to current AFA alloys.

[0126] The alloys described herein can be used in components such as engine exhaust manifolds and turbocharger housings to achieve efficiency and emission goals. The analyzed compositions of a series of exploratory lab cast AFA alloys (AFA1, AFA2, AFA3 and AFA5) and reference alloys 1.4826, HK and HP are shown in Table 1:

TABLE 1

Analyzed compositions (wt. %) of AFA alloys.

Alloy ID	Fe	Ni	Cr	Al	Cu	Mn	Mo	Nb	Si	Ti	W	Zr	Y	C	B
AFA1	50.54	25.30	15.00	4.02	0.50	1.95	<0.01	0.98	1.00	0.18	<0.01	0.09	0.04	0.37	0.01
AFA2	47.54	25.13	15.10	3.96	0.46	1.89	1.98	1.01	0.98	0.19	1.22	0.09	0.03	0.39	0.01
AFA3	49.01	25.21	15.12	4.02	0.50	1.95	<0.01	2.47	1.00	0.18	<0.01	0.09	0.03	0.39	0.01
AFA5	51.48	22.30	17.05	4.00	<0.01	1.93	0.99	0.59	0.50	<0.01	0.53	0.09	0.04	0.48	0.01
AFA5Nb1	52.27	22.0	16.7	4.06	<0.01	1.95	1.00	0.30	0.58	<0.01	0.51	0.10	0.04	0.51	0.01
AFA5Nb2	51.19	22.3	17.3	4.02	<0.01	1.99	1.04	0.43	0.57	<0.01	0.52	0.10	0.04	0.52	0.01
AFA5Nb3	51.81	21.9	16.6	4.00	<0.01	1.94	0.98	1.08	0.56	<0.01	0.50	0.10	0.04	0.51	0.01
1.4826 (reference alloy)	10.98	22.70	<0.01	0.02	0.89	—	—	1.07	—	0.04	—	—	0.36	—	0.98
HK (nominal, reference alloy)	Bal.	20	25	—	—	1	0.2	—	1	—	—	—	—	0.40	—
HP (nominal, reference alloy)	Bal.	35	25	—	—	1	0.2	—	1	—	—	—	—	0.60	—

[0127] Oxidation data for the AFA alloys are shown in FIGS. **1-4**, along with comparison data for several chromia-forming commercial alloys: 1.4826 (Fe-11Ni-22Cr base), HK (Fe-20Ni-25Cr base), and HP (Fe-35Ni-25Cr base). These figures show oxidation data as specific mass change (mg/cm^2) vs. exposure time at 900, 950 and 1000° C. in air with 10% H_2O. Exposures were conducted in 1-h cycles. FIG. **1** is a plot of oxidation data as specific mass change (mg/cm^2) vs. exposure time at 900° C. in air with 10% H_2O, with exposures conducted in 1-h cycles. FIG. **2** is a plot of oxidation data as specific mass change (mg/cm^2, isolating and enlarging 0 to 1) vs. exposure time at 900° C. in air with 10% H_2O, with exposures conducted in 1-h cycles. FIG. **3** is a plot of oxidation data as specific mass change (mg/cm^2) vs. exposure time at 950° C. in air with 10% H_2O, with exposures conducted in 1-h cycles. FIG. **4** is a plot of oxidation data as specific mass change (mg/cm^2) vs. exposure time at 1000° C. in air with 10% H_2O, with exposures conducted in 1-h cycles.

[0128] The alumina forming AFA alloys exhibited superior oxidation resistance when compared to the chromia-forming 1.4826 (Fe-11Ni-22Cr base), HK (Fe-20Ni-25Cr base), and HP (Fe-35Ni-25Cr base) commercial alloys. Despite its lower Nb content, alloy AFA 5 exhibits comparable oxidation resistance to the AFA alloys 1-3 containing higher Nb. Alloys AFA 1, 2, and 3 exhibited small positive mass changes consistent with protective alumina formation at 900 and 950° C. after 1000, 1-h cycles in air with 10% H_2O, which is a highly aggressive test condition. By comparison, the chromia-forming commercial alloys exhibited significantly worse oxidation resistance with mass loss due to both chromia volatilization and oxide scale spallation. The commercial alloys exhibited oxidation resistance in the order of their Ni and Cr content: (higher levels=better resistance but also higher cost), but even in costly HP with 35Ni and 25 Cr oxidation resistance was inadequate.

[0129] The AFA 5 alloy also exhibited small positive mass changes consistent with protective alumina formation at 900 and 950° C. after 1000, 1-h cycles in air with 10% H_2O despite its low Nb level. Continuous, protective alumina formation by AFA 5 at 950° C. was confirmed in cross-section analysis. FIG. **5** is a scanning electron microscopy (SEM) cross-section image and elemental maps of the oxide scale formed on AFA5 after 1000, 1-h cycles at 950° C. in air with 10% H_2O showing continuous scale formation. FIG. **6** is a scanning transmission electron microscopy (STEM) cross-section image of the oxide scale formed on AFA 5 after 1000, 1-h cycles at 950° C. in air with 10% H_2O showing continuous scale formation. FIG. **7** is an Al elemental map of the oxide scale formed on AFA 5 after 1000, 1-h cycles at 950° C. in air with 10% H_2O. FIG. **8** is an O elemental map of the oxide scale formed on AFA 5 after 1000, 1-h cycles at 950° C. in air with 10% H_2O. All of the AFA alloys exhibited acceptable but borderline alumina formation at 1000° C. in the aggressive cycle test, with a transition to minor mass loss and spallation over the course of the exposure.

[0130] Based on these results alloys AFA 2 and AFA 5 were down selected for additional testing. FIG. **9** shows the yield and ultimate tensile strengths of alloys at 900° C. for AFA1, AFA2, AFA3, and AFA5 and reference alloy 1.4826. AFA 2 and AFA 5 show the highest strengths in this group of alloys. Creep data for an aggressive screening condition of 900° C. and 50 MPa are shown in FIG. **10**. FIG. **10** is a bar chart showing creep rupture life (h) at 900° C. and 50 MPa for lab cast alumina-forming AFA 5 and AFA 2 relative to commercial chromia-forming 1.4826 (Fe-11Ni-22Cr base), HK (Fe-20Ni-25Cr base), and HP (Fe-35Ni-25Cr base) commercial alloys. Creep rupture life data for the chromia-formers was based on estimates from literature data. The 25 Ni-1Nb alloy AFA 2, exhibited a rupture lifetime of 421 h, comparable to the more expensive 35Ni base HP reference alloy (250 h average ±25% range based on extrapolated literature data). The HP reference alloy also exhibited inferior oxidation resistance. However, the 22 Ni-0.59 Nb alloy AFA 5 exhibited a rupture lifetime of 1181 h, nearly 3 times the lifetime of AFA 2. Therefore, AFA 5 exhibited comparable oxidation resistance but superior creep strength to AFA 2. AFA 2 contains 2 wt. % Mo and 1 wt. % W additions to improve creep resistance, in contrast to AFA 5 which contains only 1 wt. % Mo and 0.5 wt. % W, thereby resulting in AFA 5 being less expensive than AFA 2. AFA 5 also exhibited superior oxidation and creep resistance to the more costly 35 Ni base commercial HP alloy.

[0131] Table 2 below summarizes all analyzed compositions of additional alloys based on AFA5 containing variations in alloying elemental additions including Ni, Al, Si, Nb and Y.

TABLE 2

Compositions of additional invention alloys

Alloy ID	Fe	Ni	Cr	Al	Mn	Mo	Nb	Si	W	Zr	Y	C	B
AFA5Ni0	51.15	22.2	17.4	3.91	1.97	1.05	0.62	0.44	0.54	0.11	0.040	0.5100	0.0110
AFA5Ni1	53.68	20.0	17.2	3.92	1.95	1.05	0.62	0.41	0.53	0.11	0.032	0.5086	0.0133
AFA5Ni2	55.14	18.3	17.5	3.85	1.96	1.05	0.61	0.42	0.52	0.10	0.025	0.5083	0.0073
AFA5Nb1	52.27	22.0	16.7	4.06	1.95	1.00	0.30	0.58	0.51	0.10	0.035	0.5096	0.0076
AFA5Nb2	51.19	22.3	17.3	4.02	1.99	1.04	0.43	0.57	0.52	0.10	0.041	0.5191	0.0078
AFA5Nb3	51.81	21.9	16.6	4.00	1.94	0.98	1.08	0.56	0.50	0.10	0.039	0.5061	0.0067
AFA5Si1	51.207	22.0	17.0	4.00	2.00	1.00	0.60	1.00	0.50	0.10	0.083	0.5000	0.0100
AFA5Si2	50.707	22.0	17.0	4.50	2.00	1.00	0.60	1.00	0.50	0.10	0.083	0.5000	0.0100
AFA5Y1	50.69	22.4	17.6	4.00	2.06	1.01	0.63	0.54	0.50	0.10	<0.005	0.5169	0.0073
AFA5Y2	50.87	22.3	17.4	4.00	2.04	1.01	0.63	0.54	0.50	0.10	0.130	0.5185	0.0074
AFA5Y3	51.33	21.9	17.3	3.95	2.02	1.00	0.64	0.54	0.51	0.10	0.190	0.5112	0.0106
HK30Nb (Reference alloy)	50.6	20.76	24.92	0.01	0.52	0.28	1.55	0.75	0.01	<0.01	<0.005	0.0016	0.0016

[0132] FIG. **11** shows the effect of Ni content on the mass change (mg/cm^2) of selected alloys shown in Table 2 after 1000 h of exposure during cyclic oxidation testing at 950° C. in air with 10% water vapor in 1 h cycles. FIG. **11** shows larger mass losses in alloys with Ni content less than 20 wt. %.

[0133] FIG. **12** shows the mass change (mg/cm^2) after 500 h of exposure during cyclic oxidation testing at 1000° C. in air with 10% water vapor in 1 h cycles as a function of Ni content in the alloy. FIG. **12** shows increasing mass losses when the Ni content decreases below 22 wt. %.

[0134] FIG. **13** shows the mass change (mg/cm^2) after 1000 h of exposure during cyclic oxidation testing at 950° C. in air with 10% water vapor in 1 h cycles as a function of Nb content in the alloy. FIG. **13** shows that the oxidation resistance increases monotonically when the Nb content is equal to or greater than 0.4 wt. %, whereas the oxidation resistance decreases (increasing mass loss) for Nb levels less than 0.4 wt. %.

[0135] FIG. **14** shows the mass change (mg/cm^2) after 100 h of exposure during cyclic oxidation testing at 1000° C. in air with 10% water vapor in 1 h cycles as a function of Nb content in the alloy. FIG. **14** shows that the mass gain decreases and the oxidation resistance increases monotonically with increasing Nb content greater than 0.3 wt. %.

[0136] FIG. **15** shows the mass change (mg/cm^2) after 500 h of exposure during cyclic oxidation testing at 950° C. in air with 10% water vapor in 1 h cycles as a function of Al and Si contents in the alloy. FIG. **15** shows that the mass gain decreases and the oxidation resistance increases with increasing Al and Si levels. An alloy with 4.5 Al-1 Si has lower positive mass gain than an alloy with 3.9 Al-0.4 Si indicating the formation of a slower growing oxide and hence better oxidation resistance.

[0137] FIG. **16** shows the mass change (mg/cm^2) after 500 h of exposure during cyclic oxidation testing at 1000° C. in air with 10% water vapor in 1 h cycles as a function of Y content in the alloy. FIG. **16** shows that an alloy with 0 Y has significant mass loss (−126 mg/cm^2) indicating poor oxidation resistance. The mass gain becomes positive indicating improved oxidation resistance with increasing addition Oxidation test results suggested that careful control of alloying additions in the invention alloys was necessary. The results from oxidation testing at 950° C. of the commercial cast stainless alloy HK30Nb (chromia-forming cast austenitic stainless steel, Fe-20Ni-25Cr base) showed an abrupt mass loss in the early stages of oxidation testing, suggesting formation of an unprotective oxide scale under these testing conditions. In general, the invention alloys and particularly AFA 5 and related alloys demonstrated very slow oxidation kinetics at both 950 and 1,000° C., indicating highly protective alumina formation.

[0138] FIG. **17** is a bar chart showing a comparison of creep-rupture lives of cast AFA 5 alloys (lab-scale heats) and reference HK30Nb alloy tested at 900° C. and 50 MPa. FIG. **17** shows the effect of additions of Ni, Nb, Al, Si, and Y on the creep properties of the alloys shown in Table 2. The creep rupture life decreases when the Nb content increases from 0.3 wt. % (AFA5Nb1) to 1.08 wt. % (AFA5Nb3). An increase in Al and Si levels from 3.9 Al-0.44 Si to 4.5 Al-1 Si results in a decrease of the creep rupture life. An increase in Y levels from 0.04 to 0.19 also decreases the creep resistance. All AFA alloys have better creep resistance than reference alloy HK30Nb at 950° C. and 50 MPa.

[0139] Among the alloying additions, reductions of Ni and Y contents had a strong negative impact on oxidation resistance of AFA. As the Ni content reduced from 22.2 to 18.3 wt. %, the mass loss occurred earlier and more aggressively at both test temperatures. Thus, the results suggested that a minimum threshold of ~18 wt. % Ni would be acceptable. The Nb contents between 0.30 to 1.08 wt. % did not show a significant influence on the oxidation resistance at 950° C., whereas the lower Nb contents (0.30 and 0.43 wt. %) resulted in a reduced mass gain at 1,000° C. Increasing Si or Si+Al contents reduced the mass gains at 950° C. (FIG. **15**), but both of these additions showed a negative impact on creep-rupture performance (FIG. **17**). Reduction of the Y content resulted in a loss of oxidation resistance at 1,000° C. (FIG. **16**). Increasing Y additions up to 0.19 wt. % positively improved the oxidation resistance, although higher levels of Y may have a detrimental effect on room-temperature ductility.

[0140] Although many alloys show a creep rupture life greater than 1000 h at 900° C. and 50 MPa (FIG. **17**), additions of 1.08 Nb (AFA5Nb3), 0.19 Y (AFA5Y3), 1 Si (AFA5i1), and 4.5 Al+1 Si (AFA5Si2) resulted in significant reduction of creep-rupture lives. These alloying additions are considered to deteriorate the creep-strengthening mechanism proposed for the AFA 5 alloy design; (1) excess Nb addition significantly lowers the amount of the strengthening $M_{23}C_6$ phase, (2) excess Y addition introduces dispersions of a weak eutectic microstructure, and (3) excess Si addition

promotes G-phase (Ni—Nb—Si rich intermetallic compound) formation which also negatively impacts the creep-rupture performance.

[0141] FIG. **18** is a plot showing the creep rupture lives at 900° C. and 500 MPa as a function of the atomic ratio R defined by

$$R=(Ni+Cr+Mn+Mo+W+C+B)/(Al+Nb+Si+Zr+Y) \quad \text{(Eq 1)}$$

all in atomic %. FIG. **18** shows that creep rupture life at 900° C. and 500 MPa increases with increasing R with the best creep properties obtained for R greater than 4.4.

[0142] FIG. **19** is a plot showing creep-rupture lives (h) tested at 900° C. and 50 MPa, and a bar chart showing mass gains (mg/cm^2), after total 1000 h exposure at 950° C. in air with 10% water vapor environment in AFA 5 base alloys, plotted as a function of the Nb composition. FIG. **19** shows that alloys with Nb levels greater than or equal to 0.4Nb have good oxidation resistance and good creep properties (AFA5Nb2, AFANi0, and AFA5Nb3) with the creep rupture lives decreasing with increasing Nb levels.

[0143] Additional experimental results of AFA 5 base alloys with variation of the Nb content (from 0.30 to 1.08 wt. %) are shown in FIG. **19**. FIG. **19** is a plot showing creep-rupture lives (h) tested at 900° C. and 50 MPa, and a bar chart showing mass gains (mg/cm^2), after total 1000 h exposure at 950° C. in air with 10% H_2O environment in AFA 5 base alloys, plotted as a function of the Nb composition. FIG. **19** shows a lower Nb limit (~0.4Nb) from oxidation behavior whereas no lower limit in creep rupture performance. This demonstrates a lower limit of the Nb content down to 0.4 wt. % in the present invention. Creep-rupture life at 900° C. and 50 MPa increased with the Nb content as expected from computational findings in Table 3 and 4, suggesting that the lower Nb addition than 0.6 wt. % showing the improved creep performance in the invention alloys. The mass gain after the oxidation test for total 1,000 h at 950° C. in air with 10% H_2O environment increased with decreasing Nb addition is down to 0.43 wt. % Nb, indicating the Nb effect on stabilizing the protective alumina scale reduces continuously down to 0.43 wt. % Nb, although the amount of mass gain is still low enough to prove a promising oxidation resistance. The mass gain behavior appeared discontinuous between 0.30 and 0.43 wt. % Nb at 950° C. The low mass gain in the alloy with 0.3 wt. % Nb was due to a change from mass gain to mass loss during oxidation testing, suggesting that the insufficient Nb addition below a threshold led to a loss of protectiveness. Because of this transition in the oxidation behavior between 0.30 and 0.43 wt. % Nb at 950° C., in one embodiment, the alloys described herein have the lower Nb limit at 0.4 wt. % Nb.

[0144] FIGS. **20** to **35** show the calculated equilibrium phase fractions as a function of temperature for alloys shown in Table 2. FIG. **36** is a plot of mole fraction % vs. temperature (° C.) obtained for the cast AFA 5 alloy showing the phases predicted to appear during solidification. FIG. **37** is a plot of thermodynamic calculation results of the cast AFA 5 alloy series showing the amounts of equilibrated and as-solidified mole fraction % of $M_{23}C_6$. The two arrows in FIG. **37** indicate the changes in the amounts of $M_{23}C_6$ precipitation and M_7C_3 dissolution of as-solidified AFA 5 alloy exposed at 900° C., which play important roles on optimizing the creep performance of the alloy through precipitation strengthening at the designated temperature. The equilibrium and solidification calculations were performed using JMatPro®. Yttrium, boron and other minor elements were not included in the calculations. Similar calculations were performed for other alloys shown in Tables 2 and 3.

[0145] Tables 3 and 4 summarize the phases present after solidification and at equilibrium at 900° C. obtained from the results of the calculations. The carbide contents after solidification in the invention alloys are observed to range from 0.26 to 0.57 mole % (MC), 1.29 to 2.59 mole % ($M_{23}C_6$), 0.84 to 2.25 mole % (M_7C_3), and 0 to 0.02 mole % (M_6C). The total mole % of carbides is observed to be from 3.73 to 4.27. The carbide contents at equilibrium at 900° C. in the invention alloys are observed to range from 0.31 to 0.67 mole % (MC), and 9.01 to 9.86 mole % ($M_{23}C_6$), with the total mole % of carbides ranging from 9.19 to 10.24. The change in carbide contents ranges from 5.62 to 6.33 mole %.

TABLE 3

Calculated amounts of phases (mole %) after solidification and at equilibrium at 900° C. for alloys shown in Table 1

	Calculated phases after solidification, mole %								Calculated equilibrium phases at 900° C.							
Alloy ID	FCC-Fe	MC	$M_{23}C_6$	M_7C_3	M_6C	G-phase	B2-NIA1	total carbides	FCC-Fe	MC	$M_{23}C_6$	B2-NIA1	⍰	total carbides	Changes in $M_{23}C_6$-MC	Changes in total carbides
AFA1	97.65	1.19		1.16				2.35	92.80	1.42	4.31	1.47		5.73	4.54	3.38
AFA2	96.00	1.29	1.55		1.05			4.00	90.12	1.40	5.94	2.22	1.22	6.44	1.49	2.44
AFA3	97.00	2.65		0.76		0.10	0.10	2.81	93.77	1.03	1.12	2.09		4.15	1.50	1.94
AFA5	96.27	0.53	1.80	1.40				3.73	90.43	0.63	8.36	0.38		9.19	6.86	5.46
AFA5Nb1	96.17	0.26	1.29	2.25	0.02			3.83	88.81	0.31	9.86	1.02		10.16	8.61	6.33
AFA5Nb2	95.82	0.38	1.68	2.12				4.18	88.73	0.44	9.50	1.03		10.24	8.17	6.06
AFA5Nb3	96.11	1.02	1.83	1.24				3.89	90.24	1.16	7.95	0.64		9.12	6.47	5.23

⍰ indicates text missing or illegible when filed

TABLE 4

Calculated amounts of the phases (mole %) after solidification and at equilibrium at 900° C. for alloys shown in Table 2

	Calculated phases after solidification, mole %							Calculated equilibrium phases at 900° C.							Changes
Alloy ID	FCC-Fe	MC	$M_{23}C_6$	M_7C_3	M_6C	BCC-Cr	total carbides	FCC-Fe	MC	$M_{23}C_6$	B2-NIA1	Sigma	total carbides	Changes in $M_{23}C_6$-MC	in total carbides
AFA5Ni0	95.83	0.56	2.23	1.37			4.17	90.22	0.67	9.12			9.78	6.99	5.62
AFA5Ni1	96.03	0.56	2.30	1.11			3.97	90.30	0.67	9.03			9.70	6.83	5.73
AFA5Ni2	96.02	0.55	2.59	0.84			3.98	90.33	0.66	9.01			9.67	6.53	5.69
AFA5Nb1	96.17	0.26	1.29	2.25	0.02		3.83	88.81	0.31	9.86	1.02		10.16	8.61	6.33
AFA5Nb2	95.82	0.38	1.68	2.12			4.18	88.73	0.44	9.80	1.03		10.24	8.17	6.06
AFA5Nb3	96.11	1.02	1.63	1.24			3.89	90.24	1.16	7.95	0.64		9.12	6.67	5.23
AFA5Si1	95.88	0.55	0.93	2.36	0.29		4.12	87.53	0.50	8.99	2.89		9.59	8.11	5.46
AFA5Si2	95.84	0.55	0.43	2.78	0.41		4.16	84.09	0.54	9.08	6.29		9.62	8.64	5.45
AFA5Y1	95.73	0.57	1.94	1.76			4.27	89.17	0.65	9.26	0.91		9.92	7.41	5.64
AFA5Y2	95.80	0.57	1.84	1.79			4.20	89.24	0.66	9.28	0.82		9.94	7.53	5.74
AFA5Y3	95.91	0.58	1.89	1.62			4.09	89.87	0.68	9.08	0.37		9.76	7.29	5.67
HK30Nb	85.99	1.42	0.73			11.86	2.15	94.96	1.67	2.58		0.79	4.25	2.11	2.11

[0146] Table 5 shows the creep rupture life of the invention alloys at 900° C. 50, MPa, h and Mass gain (in air with 10% water vapor, 1 h cycle), mg/cm 3, after 500 h and 1000 h at 950° C., and 100 h and 500 h at 1000° C., and Atomic ratio R calculated using Eq. 1.

TABLE 5

Creep rupture life at 900° C. 50, MPa, h and Mass gain (in air with 10% water vapor, 1 h cycle), mg/cm^3, and Atomic ratio using Eq. 1

		Mass gain (in air - 10% water vapor, 1 h cycle), mg/cm^3				
Alloy ID	Rupture life at 900° C., 50 MPa, h	950° C., total 500 h	950° C., total 1,000 h	1000° C., total 100 h	1000° C., total 500 h	Atomic ratio in Eq. 1
AFA5Ni0	1182	0.35	0.47	0.29	0.54	4.77
AFA5Ni1	1368		0.12		−1.06	4.54
AFA5Ni2	1160		−8.86		−13.36	4.47
AFA5Nb1	1428		0.34	0.38	0.40	4.48
AFA5Nb2	1142		0.55	0.33	0.41	4.59
AFA5Nb3	782		0.39	0.35	0.57	4.32
AFA5Si1	694	0.27				4.13
AFA5Si2	373	0.27				3.77
AFA5Y1	1337				−129.48	4.64
AFA5Y2	1240				0.50	4.57
AFA5Y3	917				0.38	4.55
HK30Nb	123, 127, 143	−26.07				N.A.

[0147] The invention can potentially increase the upper-temperature oxidation limit to ≥900-950° C. for next generation cast austenitic stainless steel exhaust gas components. Candidate alloys will utilize an Fe(Ni) base with ≤25-30 wt. % Ni to remain cost competitive, as well as minimize the use of other costly alloying additions, such as Mo, Nb, W, etc. The cast stainless alloys of the invention form an alumina (Al_2O_3) protective oxide scale on the surface during oxidation rather than the chromia (Cr_2O_3) oxide scales that form on most commercial stainless alloys. Alumina scales are typically slower growing and more protective than chromia scales, particularly at higher temperatures, but alloy design and the casting of Al-containing stainless alloys can be challenging.

[0148] The invention as shown in the drawings and described in detail herein disclose arrangements of elements of particular construction and configuration for illustrating preferred embodiments of structure and method of operation of the present invention. It is to be understood however, that elements of different construction and configuration and other arrangements thereof, other than those illustrated and described may be employed in accordance with the spirit of the invention, and such changes, alternations and modifications as would occur to those skilled in the art are considered to be within the scope of this invention as broadly defined in the appended claims. In addition, it is to be understood that the phraseology and terminology employed herein are for the purpose of description and should not be regarded as limiting.

We claim:

1. An AFA alloy composition comprising:
0.4 to 0.59 Nb+Ta;
0.4 to 0.6 C;
16 to 18 Cr;
18-23 Ni;
3.5-5.5 Al;
0.005 to 0.15 B;
up to 1.5 Mo;
up to 2 Co;
up to 1 W;
up to 3 Cu;

up to 4 Mn;
up to 2 Si;
up to 0.5 wt. % total of at least one element selected from the group consisting of Ti and V;
up to 0.06 N;
up to 1 wt. % total of at least one element selected from the group consisting of Y, La, Ce, Hf, and Zr;
balance Fe, wherein the weight percent Fe is greater than the weight percent Ni, and wherein said alloy forms an external continuous scale comprising alumina to at least 900° C. in air with 10% H_2O, and a stable essentially single phase FCC austenitic matrix microstructure, said austenitic matrix being essentially delta-ferrite free and essentially BCC-phase-free, with creep rupture life in excess of 500 h at 900° C. and 50 MPa.

2. The alloy of claim **1**, wherein the alloy has a creep rupture life greater than 1000 h at 900° C. and 50 MPa.

3. The alloy of claim **1**, wherein the alloy has a yield strength at 900° C. that is greater than 18.75 ksi.

4. The alloy of claim **1**, wherein the alloy has a yield strength at 900° C. that is greater than 21 ksi.

5. The alloy of claim **1**, wherein the alloy has a ultimate tensile strength is greater than 22.75 ksi.

6. The alloy of claim **1**, wherein the alloy has a ultimate tensile strength is greater than 26 ksi.

7. The alloy of claim **1**, wherein the mass gain after exposure to air with 10 vol % H_2O at 950° C. in 1 h cycles for 1000 h is less than 1 mg/cm^2.

8. The alloy of claim **1**, wherein the mass gain after exposure to air with 10 vol % H_2O at 1000° C. in 1 h cycles for 500 h is less than 1 mg/cm^2.

9. The alloy of claim **1**, wherein the atomic ratio R can be from 3.77 to 4.77.

10. The alloy of claim **1**, wherein the atomic ratio R can be from 4.42 to 4.77.

11. The alloy of claim **1**, wherein the calculated equilibrium mole % at 900° C. of MC carbides is from 0.31 to 0.67.

12. The alloy of claim **1**, wherein the calculated equilibrium mole % at 900° C. of $M_{23}C_6$ carbides is from 8.56 to 9.86.

13. The alloy of claim **1**, wherein the calculated equilibrium mole % at 900° C. of MC and $M_{23}C_6$ carbides is from 9.19 to 10.24.

14. The alloy of claim **1**, wherein the calculated change in mole % of total carbides after exposure to 900° C. is from 5.46 to 6.33.

15. The alloy of claim **1**, wherein the calculated change in mole % of MC and $M_{23}C_6$ after exposure to 900° C. is from 6.86 to 8.61.

16. The alloy of claim **1**, wherein the alloy consists essentially of:
0.4 to 0.59 Nb+Ta;
0.4 to 0.6 C;
16 to 18 Cr;
18-23 Ni;
3.5-5.5 Al;
0.005 to 0.15 B;
up to 1.5 Mo;
up to 2 Co;
up to 1 W;
up to 3 Cu;
up to 4 Mn;
up to 2 Si;
up to 0.5 wt. % total of at least one element selected from the group consisting of Ti and V;
up to 0.06 N;
up to 1 wt. % total of at least one element selected from the group consisting of Y, La, Ce, Hf, and Zr;
balance Fe, wherein the weight percent Fe is greater than the weight percent Ni, and wherein said alloy forms an external continuous scale comprising alumina to at least 900° C. in air with 10% H_2O, and a stable essentially single-phase FCC austenitic matrix microstructure, said austenitic matrix being essentially delta-ferrite free and essentially BCC-phase-free, with creep rupture life in excess of 500 h at 900° C. and 50 MPa.

17. The alloy of claim **1**, wherein the alloy consists of:
0.4 to 0.59 Nb+Ta;
0.4 to 0.6 C;
16 to 18 Cr;
18-23 Ni;
3.5-5.5 Al;
0.005 to 0.15 B
up to 1.5 Mo
up to 2 Co;
up to 1 W;
up to 3 Cu;
up to 4 Mn;
up to 2 Si;
up to 0.5 wt. % total of at least one element selected from the group consisting of Ti and V;
up to 0.06 N;
up to 1 wt. % total of at least one element selected from the group consisting of Y, La, Ce, Hf, and Zr;
balance Fe, wherein the weight percent Fe is greater than the weight percent Ni, and wherein said alloy forms an external continuous scale comprising alumina to at least 900° C. in air with 10% H_2O, and a stable essentially single-phase FCC austenitic matrix microstructure, said austenitic matrix being essentially delta-ferrite free and essentially BCC-phase-free, with creep rupture life in excess of 500 h at 900° C. and 50 MPa.

* * * * *